②

AD-A219 543

NAVAL POSTGRADUATE SCHOOL
Monterey, California

DTIC
D

THESIS

A CASE STUDY OF EXPLOSIVE CYCLOGENESIS
IN THE EASTERN PACIFIC OCEAN
14-17 DECEMBER 1987

by

Jan Curtis

September 1989

Thesis Advisor   C.H. Wash

90 03 26 048

REPORT DOCUMENTATION PAGE

Form Approved
OMB No. 0704-0188

1a REPORT SECURITY CLASSIFICATION Unclassified	1b RESTRICTIVE MARKINGS

2a. SECURITY CLASSIFICATION AUTHORITY	3 DISTRIBUTION/AVAILABILITY OF REPORT
2b. DECLASSIFICATION/DOWNGRADING SCHEDULE	Approved for public release; distribution is unlimited.

4. PERFORMING ORGANIZATION REPORT NUMBER(S)	5 MONITORING ORGANIZATION REPORT NUMBER(S)

6a NAME OF PERFORMING ORGANIZATION Naval Postgraduate School	6b OFFICE SYMBOL (If applicable) 35	7a. NAME OF MONITORING ORGANIZATION Naval Postgraduate School

6c. ADDRESS (City, State, and ZIP Code) Monterey, CA 93943-5000	7b ADDRESS (City, State, and ZIP Code) Monterey, CA 93943-5000

8a. NAME OF FUNDING/SPONSORING ORGANIZATION	8b OFFICE SYMBOL (If applicable)	9 PROCUREMENT INSTRUMENT IDENTIFICATION NUMBER

8c. ADDRESS (City, State, and ZIP Code)	10 SOURCE OF FUNDING NUMBERS			
	PROGRAM ELEMENT NO	PROJECT NO	TASK NO	WORK UNIT ACCESSION NO.

11 TITLE (Include Security Classification) A Case Study of Explosive Cyclogenesis in the Eastern Pacific Ocean 14-17 December 1987

12. PERSONAL AUTHOR(S) Jan Curtis

13a TYPE OF REPORT Master's Thesis	13b TIME COVERED FROM _____ TO _____	14 DATE OF REPORT (Year, Month, Day) 1989, September	15 PAGE COUNT 69

16 SUPPLEMENTARY NOTATION

17 COSATI CODES			18 SUBJECT TERMS (Continue on reverse if necessary and identify by block number)
FIELD	GROUP	SUB-GROUP	Explosive cyclogenesis, marine cyclogenesis.

19. ABSTRACT (Continue on reverse if necessary and identify by block number)

An explosive cyclogenesis event that occurred in the eastern Pacific Ocean on 14-17 December 1987 is investigated using the National Meteorological Center (NMC) final analyses and Geostationary Operational Environmental Satellite (GOES) digital imagery. Forecasts for this cyclone by the Navy Operational Global Atmospheric Prediction System (NOGAPS 3.0) and NMC Nested Grid Mesh (NGM) forecasts initialized at 12 UTC 14 December are also evaluated. Qausi-Langrangian budgets of mass and vorticity are computed to understand the factors responsible for the development of this intense cyclone.

The initial surface development occurs within a strong baroclinic southeast of a significant short-wave trough aloft. Rapid intensification is accompanied by large cyclonic vorticity advection in the upper troposphere as the surface cyclone moves under the divergent quadrant of a 250 mb jet streak. A key element in this development is the superposition between the pre-existing surface low and upper level short-wave trough in a favorable weak static stability environment. These observations support earlier

20 DISTRIBUTION/AVAILABILITY OF ABSTRACT ☒ UNCLASSIFIED/UNLIMITED ☐ SAME AS RPT ☐ DTIC USERS	21 ABSTRACT SECURITY CLASSIFICATION Unclassified
22a NAME OF RESPONSIBLE INDIVIDUAL Carlyle H. Wash	22b TELEPHONE (Include Area Code) (408)646-2295	22c OFFICE SYMBOL 63Wx

DD Form 1473, JUN 86   Previous editions are obsolete   SECURITY CLASSIFICATION OF THIS PAGE

S/N 0102-LF-014-6603

i

19.(continued)

studies that upper level forcing acts as a critical catalyst in initiating eastern ocean explosive development.

A Case Study of Explosive Cyclogenesis
in The Eastern Pacific Ocean
14-17 December 1987

by

Jan Curtis
Lieutenant Commander, United States Navy
B.S., City College of New York, 1974

Submitted in partial fulfillment of the
requirements for the degree

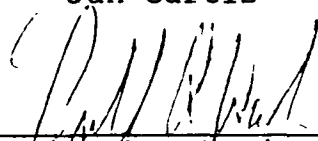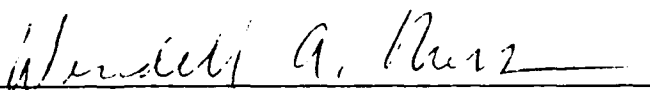MASTER OF SCIENCE IN METEOROLOGY AND OCEANOGRAPHY

from the

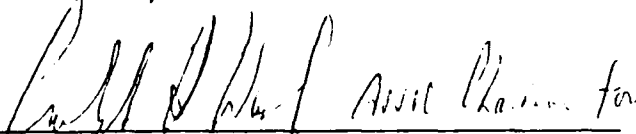NAVAL POSTGRADUATE SCHOOL
September 1989

Author: _____
                    Jan Curtis

Approved by: _____
                    C.H. Wash, Thesis Advisor

_____
W.A. Nuss, Second Reader

_____
Robert J. Renard, Chairman
Department of Meteorology

Abstract

An explosive cyclogenesis event that occurred in the eastern Pacific Ocean on 14-17 December 1987 is investigated using the National Meteorological Center (NMC) final analyses and Geostationary Operational Environmental Satellite (GOES) digital imagery. Forecasts for this cyclone by the Navy Operational Global Atmospheric Prediction System (NOGAPS 3.0) and NMC Nested Grid Mesh (NGM) forecasts initialized at 12 UTC 14 December are also evaluated. Quasi-Lagrangian budgets of mass and vorticity are computed to determine the factors responsible for the development of this intense cyclone.

The initial surface development occurs within a strong baroclinic zone southeast of a significant short-wave trough aloft. Rapid intensification is accompanied by large cyclonic vorticity advection in the upper troposphere as the surface cyclone moves under the divergent quadrant of a 250mb jet streak. A key element in this development is the superposition between the pre-existing surface low and upper level short-wave trough in a favorable weak static stability environment. These observations support earlier studies that upper level forcing acts as a critical catalyst in initiating eastern ocean explosive development.

TABLE OF CONTENTS

A-1

LIST OF TABLES

LIST OF FIGURES

I. INTRODUCTION

Today, one of the greatest challenges facing meteorologists is their ability to forecast explosive extratropical cyclogenesis. What makes this particular weather event uniquely different is the rapid rate in which an open wave appears to develop spontaneously and intensify to storm force, usually within 36 hours. Besides the obvious impact to all forms of shipping (Gyakum, 1983a) tremendous destruction of coastal structures can also result as witnessed by the 16-17 January 1988 storm which struck southern California (Ludlum, 1988) and Storm Data (National Oceanic Atmospheric Administration, 1988). Damage can extend inland several hundreds of miles and paralyze large areas. The 18-20 February 1979 Presidents' Day snowstorm, which struck the middle Atlantic States (Bosart, 1981; Bosart and Lin, 1984 and Uccellini, et al. 1984, 1985) is an excellent example of the impact of these major cyclones.

Current operational numerical weather prediction models have made great strides in predicting explosive development in recent years as reported by Uccellini, et al. (1987); Leslie, et al. (1987); Liou and Elsberry (1987) and Anthes, et al. (1983). Improved model resolution and better treatment of boundary-layer fluxes stand out as the most important contributing factors for this success (Sanders, 1987). The modelers' greatest obstacle in achieving exacting results are consistently traced back to the inaccuracies in the initialized meteorological fields (Hales,

1

Jr., 1979) and to the limited spatial resolution in the data (Sanders, 1986b, 1987b; and Leslie, et al., 1987). This latter issue was clearly demonstrated by the recent forecast success of Kuo and Reed (1988). They showed that when their controlled experiment was conducted on a 1981 storm using surface fluxes, friction and the explicit prediction of water vapor, cloud and rain water, surface development exceeded the rate of 1 mb h^{-1} for 24 h normalized geostrophically from 60 degrees latitude (one Bergeron). Although their result falls 19 mb short of the actual observed pressure of 950 mb, it proved to be substantially better than the 55 mb pressure error based on the operational Limited Fine Mesh (LFM) model 24-h surface prognosis. They also showed that when they included supplemental subjective sounding data, their model improved the storm's central pressure forecast by 11 mb.

While meteorologists cannot overlook the importance of the initialization problem on weather prediction, an equally urgent issue concerns the cause and effect relationships (synergistic interactions) between the dynamic forcing processes and circulation patterns. Increasing evidence suggests that explosive cyclogenesis is linked in particular to the planetary-scale where the interactions of large and small scale forcing are teleconnected (Namias, 1987). Additionally, recent studies show this phenomena occurs under various types of synoptic regimes where different physical processes can either reinforce or suppress development. If we are to further our understanding of

2

these important weather episodes, additional research is
essential.

Since the definition of a rapidly deepening cyclone (a
central pressure fall of at least one Bergeron) was first
popularized by Sanders and Gyakum (1980), a number of researchers
have pursued different approaches for investigating the specific
mechanisms which explain the nature of these systems. Table 1
summarizes climatological, composite and individual case studies
on explosive cyclones during the last decade. A review of Table
1 lists current results on rapid deepening.

1. There are three basic synoptic patterns associated with
   development:

   a. A zone of low level maximum baroclinicity exists
       under a nearly straight upper current which is
       influenced by upper evel forcing (i.e. jet streak
       dynamics or the passage of a weak 500 mb short
       wave trough which couples with the planetary
       boundary layer below) (Uccellini, 1986 and Wash et
       al., 1988). This a modification to Petterssen's
       A-Type development (Petterssen and Smebye, 1971).

   b. The Petterssen B-type development (Petterssen and
       Smebye, 1971) begins when a pre-existing upper
       trough, with strong vorticity advection on its
       forward side, spreads over a low-level area of
       warm or neutral advection in a region of shallow
       baroclinicity (Bosart and Lin, 1984 and Uccellini,
       et al., 1984).

   c. Development of the cold airmass cyclones (polar
       lows) is strongly influenced by reduced static
       stability due to latent heat release (Mullen,
       1983).

2. Most events occur in the cold season, over the ocean,
   about 640 km down stream of a mobile 500 mb trough and
   are within or poleward of the jet stream (Sanders and
   Gyakum, 1980).

3. Growth is due primarily to baroclinic instablity and
   indirectly to convective instability. Enhanced diabatic

processes over strong sea surface temperature (SST) gradients and Arctic air mass outbreaks over warm water appear to be responsible for the high frequency of explosive events in western oceans. Examination of satellite imagery shows that explosive cyclogenesis is accompanied by a rapid expansion of the major shield cloud north and east of the developing low.

4. Many of the forcing mechanisms are interrelated. For example, low level ageostropic flow has been found to be embedded in the indirect circulation associated with the subtropical jet and is influenced by planetary boundary layer (PBL) and diabatic processes Uccellini et al. (1987). Also, Mullen (1983) noted a simultaneous decrease in wavelength and increase in amplitude of the thermal perturbation with the onset of rapid deepening. Another nonlinear effect such as low surface roughness over the ocean is thought to favor rapid development by increasing surface convergence Sanders and Gyakum (1980).

In contrast Table 2, which summarizes numerical studies, quickly shows that there is less concensus as to the probable cause of explosive events. These differences can be explained in part as the result of the unique differences found in the initial conditions as discussed above. For example, surface energy fluxes are more important over western oceans when development occurs over strong SST gradients Anthes, et al. (1983) while convective parameterization may play a less significant role than, condensational heating over eastern oceans Kuo and Reed (1988). There is general agreement that reducing grid size beyond 45 km results in little improvement in the storm's forecast position and intensity and the addition of supplemental data substantially improves the predictions.

Nearly all explosive cyclone case studies have been focused on western ocean events. This study will concentrate on a case of explosive maritime cyclogenesis over the Northeast Pacific

TABLE 1
EXPLOSIVE CYCLOGENESIS DIAGNOSTIC STUDIES

A	1	2	3	4	5	6	7	8	9	10	11	12	13	14	15
B	M	M	MT	MP	P	P	P	S	S	S	S	S	S	S	S
C	B	P	B	A	B	A	S	A	A	P	A	A	A*	P	B
D	C	C	C	AB	AB	B	B	B	A	P	B	B	A*	A	A*P*
E	BC	B	BC	BC	BC	B	B	C?	BC	BC	B	B	B	BC	BC
F	Y	-	-	-	Y	-	Y	I	Y	I	Y	Y	-	Y	Y
G	-	-	-	-	Y	-	-	Y	-	-	Y	Y	Y	Y	Y
H	-	-	-	-	Y	-	-	-	-	-	-	#	-	Y	Y
I	Y	-	-	-	-	-	Y	Y	Y	Y	-	Y	-	Y	Y

LEGEND: Y=Important, I=Indirect, ?=Questionable

A. Authors:
    1) Sanders and Gyakum, 1980.
    2) Murty, et al., 1983.
    3) Roebber, 1984.
    4) Sanders, 1986 a,b.
    5) Rogers and Bosart, 1986.
    6) Sanders, 1987a.
    7) Holland, et al., 1987.
    8) Bosart, 1981.
    9) Gyakum, 1983a.
  10) Mullen, 1983.
  11) Bosart and Lin, 1984.
  12) Uccellini, et al., 1984, 1985.
  13) Uccellini, 1986.
  14) Reed and Albright, 1986.
  15) Wash, et al., 1988.

B. Study: M=Climatological, T=Statistical, P=Composite, S=Case

C. Region: A=North Atlantic, P=North Pacific, B=Both Oceans, S=Southwest Pacific

D. Pattern: A=Petterssen A-Type, B=Petterssen B-Type, P=Polar Low, C=All Types, *=Modified

E. Instability Mechanism: B=Baroclinic, C=Convective

F. Diabatic (latent and sensible heat flux)

G. Jet Dynamics (tropopause folding and horizontal mass divergence)

H. Weak Stability (static, symmetric): #=Important although catalyst is uncertain

I. Convection (significant signature on satellite imagery)

TABLE 2
EXPLOSIVE CYCLOGENESIS NUMERICAL STUDIES 1983-1988

A	1	2	3	4	5		A	1	2	3	4	5
B	A	A	P	S	P		G	45	-	80	$	-
C	A*	B*	A	A	A		H	&	-	N	Y	-
D	Y	?	?	-	Y		I	Y	Y	-	-	-
E	Y	-	Y	-	-		J	#	?	-	-	Y
F	Y	?	N	Y	?		K	-	-	50	-	75

LEGEND: Y=Important, N=Not important, ?=Uncertain

A. Authors: 1) Anthes et al., 1983.
              2) Uccellini, et al., 1987.
              3) Kuo and Reed, 1988.
              4) Leslie et al.,1987.
              5) Liou and Elsberry, 1987

B. Region: A=North Atlantic, P=North Pacific, S=Southwest Pacific

C. Pattern: A=Petterssen A-Type, B=Petterssen B-Type, *=Modified

D. Initialization: (model performance, a function of data accuracy)

E. Supplemental Data: (a function of data resolution)

F. Surface Energy Fluxes: (sensible heating, a function of low-level stability and moisture)

G. Resolution: Grid size in km with no significant improvement beyond this limit ($=mesoscale resolution required to capture development)

H. Cumulus Parameterization: (&=produced a stronger system but greater positional error)

I. Planetary Boundary Layer: (turbulent mixing, a function of vertical resolution)

J. Latent Heating: specifically due to shallow precipitation (#=important in later stages of development)

K. Dry Dynamics: model run without initial moisture fields (percent effected)

Ocean during the period of 14-17 December 1987. This system was selected because it showed similarities to the 13 November 1981 eastern Pacific Ocean case study by Reed and Albright (1986). Both systems developed within a strong baroclinic zone, over cool water and over a weak SST gradient. Development of these storms also occurred in regions of relatively frequent rapid cyclogenesis for the eastern Pacific Ocean Sanders and Gyakum (1980) and Roebber (1984). These frequencies are still significantly less than the rate of occurrence in western oceans. Both systems exhibited nearly identical surface pressure deepening and decay profiles (although the Reed and Albright system deepened twice as much) while synoptically resembling a modified Petterssen A-type pattern.

The Fleet Numerical Oceanography Center (FNOC) analyses of 12 UTC 14 December and 72 h forecast to 12 UTC 17 December (TAU 72) at 12 h intervals using the Navy Operational Global Atmospheric Prediction System (NOGAPS 3.0) were also investigated. This new model version consists of a multivariate optimum interpolation analyses, nonlinear normal mode initialization, and an 18 level, T47 spectral forecast model.

The main objectives of this thesis are:

1. Synoptic investigation of the rapid frontal wave cyclogenesis over the Northeast Pacific Ocean;

2. Synoptic assessment of the validity of the initialized data used in operational numerical weather prediction (NWP) models;

3. Diagnostic investigation of the maritime cyclone dynamics through the storm-centered budget analyses of mass and vorticity.

7

The approach in this thesis is similar to that of Calland (1983), Cook (1983) and Soper (1987). Final analyses fields from the National Meteorological Center (NMC) are used to examine mass and vorticity budgets for the system. Quasi Lagrangian diagnostics, as developed by Johnson and Downey (1975) and Johnson and Wash (1979), describes quantitatively cyclone development and the processes forcing changes in the circulation. The fluctuations of meteorological variables are analyzed through the use of a cylindrical budget volume centered on and translating with the surface cyclone center. Vertical and lateral exchanges and internal sources and sinks of vorticity during cyclone development are then calculated (for additional description, see Wash, et al., 1988).

II. SYNOPTIC DISCUSSION

A. Synoptic Overview

This section describes the synoptic structure of the 14-17 December 1987 cyclone using the NMC 2.5° final grid point analyses, Geostationary Operational Environmental Satellite (GOES)-WEST imagery and all available surface observations. Following this synoptic overview, a summary of two model forecasts of the cyclone are evaluated.

The storm track (Fig. 1) represents a best-fit based on post analyses and supplemental data provided by FNOC. The FNOC SST analysis for 15 December shows the storm's movement paralleling the 14°C (287°K) and 16°C (289°K) isotherms throughout most of its life. The strongest temperature gradient near the developing low is associated with a relatively weak ocean front lying several hundred kilometers to the south and represents normal climatology for early winter. This also compares very closely to the observed initial SST distribution of Reed and Albright (1986).

This explosive event is characterized by four distinct periods:

1. Open wave/weak closed circulation phase (12-18 UTC 14 December);

2. Explosive cyclogenesis phase (18 UTC 14 December-00 UTC 16 December);

3. Quasi steady-state or mature phase (00-12 UTC 16 December);

4. Dissipation phase (12 UTC 16 December-18 UTC 17

December).

These phases are clearly illustrated by the evolution of the

cyclone's central pressure in Fig. 2 and follows a similar

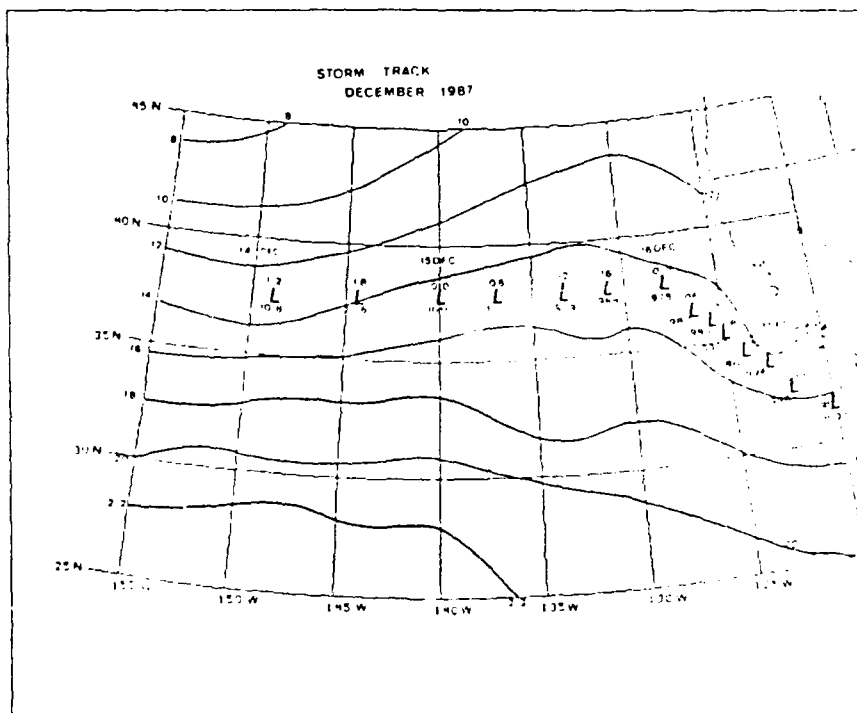profile found by the Rogers and Bosart (1986) nine year composite

study.

Fig. 1   Storm track for eastern North Pacific Ocean
Cyclone superimposed on Fleet Numerical Oceanography
Center sea surface temperature analysis (^{O}C). Cyclone
positions times are in UTC.
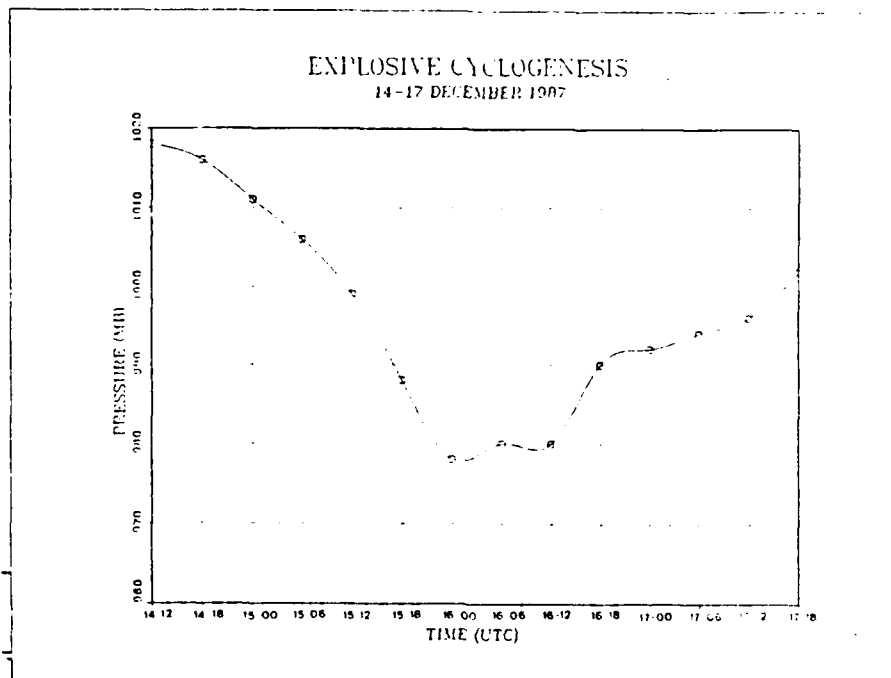
EXPLOSIVE CYCLOGENESIS
14-17 DECEMBER 1987

Fig. 2   Surface pressure trace 14-17 December 1987
based on subjective analysis.

Fig. 3 presents the mean sea-level (MSL) pressure and 1000-
500 mb thickness analyses for 12 UTC 14 December when the
incipient low is located near 37.5°N, 148.5° positioned mid-way
along a baroclinic zone which extends along 40.0°N. This frontal
boundary lies between a 1033 mb high near 47.0.° N, 149.0°W and a
1030 mb high near 32.0.°N, 134.0°W. The slowly developing low
moves east at an average speed of 15 ms^{-1}. The cyclone initially
forms at 12 UTC 14 December spontaneously on an inverted trough
associated with a strong closed cyclonic circulation 1100 km
west-northwest of the Hawaiian Islands. Elsewhere, a weakening
low east of the Alaskan panhandle with its associated cold front
trailing southward to a position just west of the Pacific
Northwest States, provides only weak thermal advection below 700

11

mb over the Gulf of Alaska. The same weak thermal advection pattern exists over the remainder of the eastern Pacific Ocean. A rapidly intensifying low near 48.0°N, 170.0°E dominates the central North Pacific Ocean. This system will amplify the meridional flow across the region during the next 24 h.

The mid-troposphere is described by the 500 mb height and absolute vorticity analysis (Fig. 4). West of the surface wave is an upper level short-wave trough and cyclonic vorticity center (CVC) (19×10^{-5}s^{-1}) extending from 40.0°N to 53.0°N along 160.0°W. Elsewhere, a second CVC (also 19×10^{-5}s^{-1}) is located near 49.0°N, 170.0°E and associated with the explosive deepening low southeast of Kamchatka. Two ridges are present over the North Pacific Ocean.
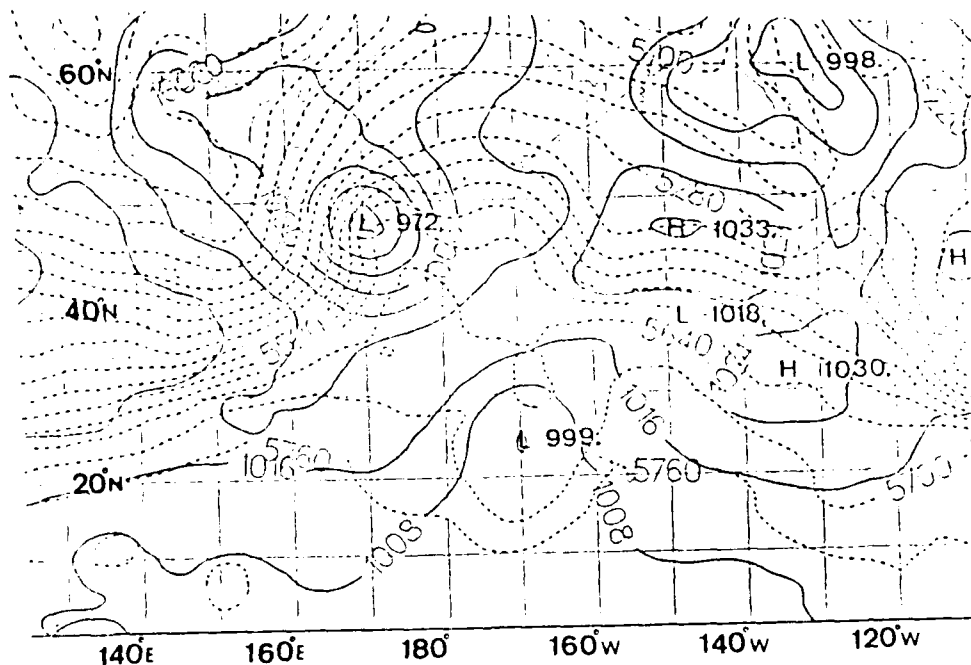

Fig. 3   National Meteorological Center grid point data analysis of MSL pressure (mb) and 500-1000 mb thickness (dm) on 12 UTC 14 December 1987 Cyclone under study is at 37.5°N 148.0°W.
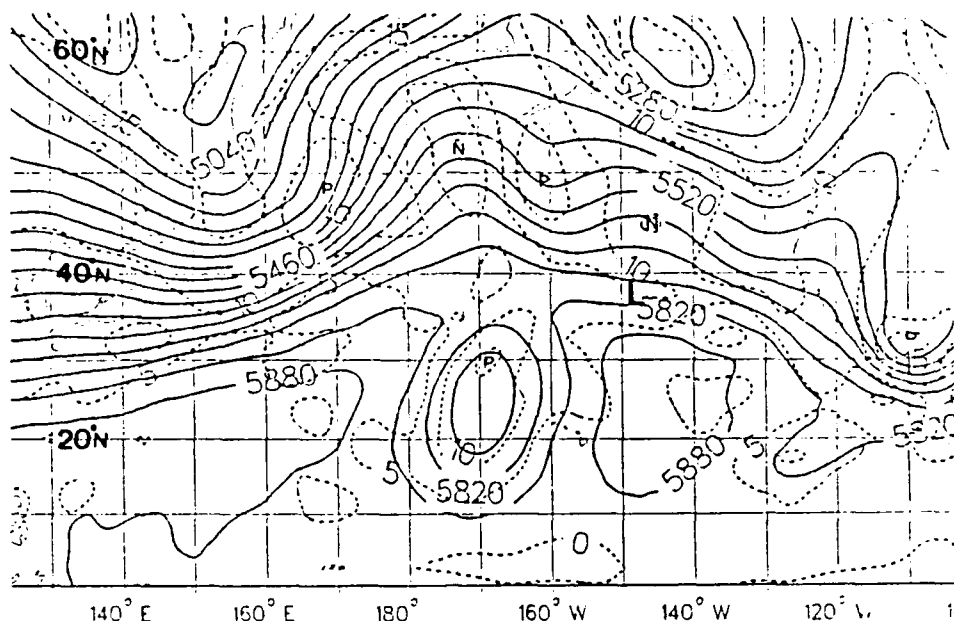
12

Fig. 4   National Meteorological Center grid point data analysis on 12 UTC 14 December 1987 of 500 mb geopotential and absolute vorticity ($10^{-5}s^{-1}$) Cyclone under study is at 37.5°N 148.0°W.

One is located between the two short wave troughs at 175.0°W while the other is north of the incipient cyclone. The cut-off low northwest of the Hawaiian Islands dominates the subtropical North Pacific Ocean.

The 250 mb wind barbs and isotach analysis (Fig. 5) describes the upper tropospheric flow. A 250 mb jet streak with maximum winds of 70ms^{-1} lies 290 km north of the incipient low. Past history of the jet streak shows that it first appeared near 50.0°N, 150.0°W sixty hours earlier as a result of the strengthening low level baroclinic zone near the incipient low. A sharp trough is present in the wind field associated with the low latitude cut-off low near 24.0°N, 170.0°W. An 85 ms^{-1} jet

13

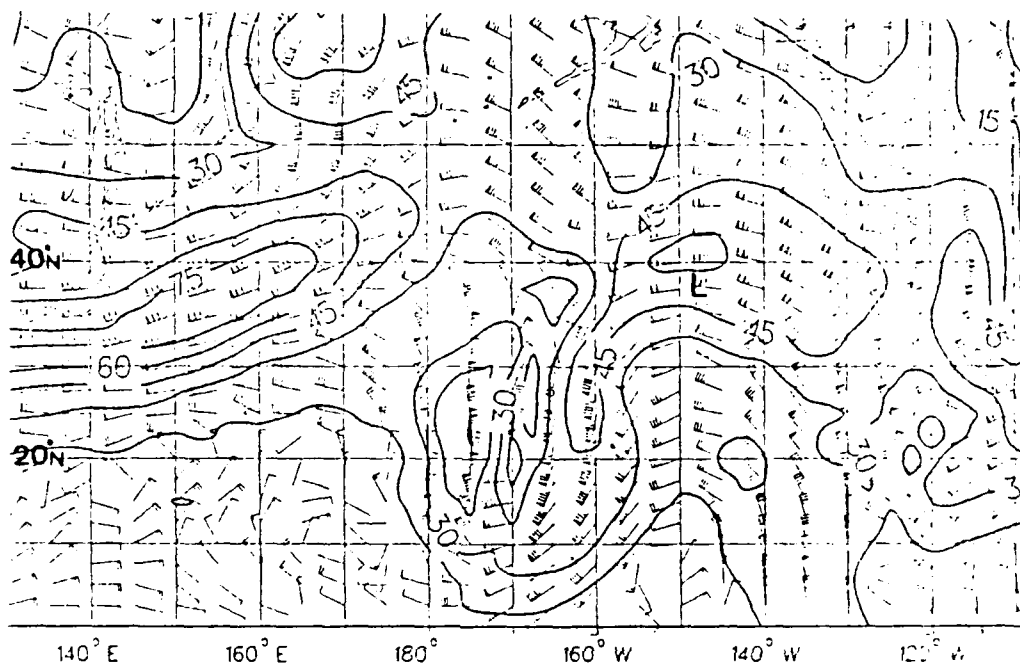streak just east of Japan is the major feature over the western

North Pacific Ocean.

Fig. 5   National Meteorological Center grid point data
analysis on 12 UTC 14 December 1987 of 250 mb wind
barbs (flag, 5ms^{-1}; pennant 25ms^{-1}) and isotachs (ms^{-1})
Cyclone under study is at 37.5^{O}N 148.0^{O}W.

The cloud pattern of this developing situation is provided

by the GOES-WEST imagery (Fig. 6). The 500 mb trough at 150.0^{O}W

is associated with a comma shaped cloud feature near 45.0^{O}N,

150.0^{O}W. The incipient low cannot be discerned in this image but

is located in the northeast-southwest cloud band as noted in Fig.

3. The short-wave cloud band is linked to a major cloud pattern

associated with the low latitude cut-off low.

At this juncture, it is interesting to note that the

incipient cyclone is south of the comma cloud pattern. Satellite

imagery rules would suggest the surface low is further to the

north. The questionable accuracy of the analyses is further evident by noting that the CVA area 160.0°-150.0°W in Fig. 4 is displaced from the multi-layer clouds located at 150.0°-140.0°W. This also suggests poor trough placement and probable weakness in its depiction (since the comma cloud is beginning to form).

Twelve hours later, 00 UTC 15 December, a subjective analysis of the developing low (Fig. 7) shows that it has deepened 7 mb since the earlier synoptic chart and is now a closed circulation. It should be noted that at this stage of development, it is common for developing mid-latitude oceanic cyclones to be poorly identified. Initial weather reports from ships, usually absent, become suddenly abundant when a system attains gale force intensity. This cyclone proved to be no exception. Relative pressure tendencies from ship reports were adjusted by taking the resultant vector between a ship's course and speed and the cyclone's moving center. This ensured that the final analyzed MSL pressure of the cyclone was consistent between synoptic periods. The substantial 3-h falling pressure tendencies to the north and east of the low are attributed to the combined eastward movement of the system and westward tracks of the ships.

The NMC objective analysis (Fig. 8) depicts the incipient cyclone with a closed 1016 mb isobar on the southern side of the baroclinic zone and agrees with the subjective analysis in Fig. 7. The western North Pacific Ocean cyclone, located at $53.^\circ$N, 174°E, deepens 26 mb in 12 h to a central pressure of 946 mb.

Other features of note include the distinct thermal trough at 150.0°W west of the incipient low and the cut-off low near Hawaii filling 5 mb.

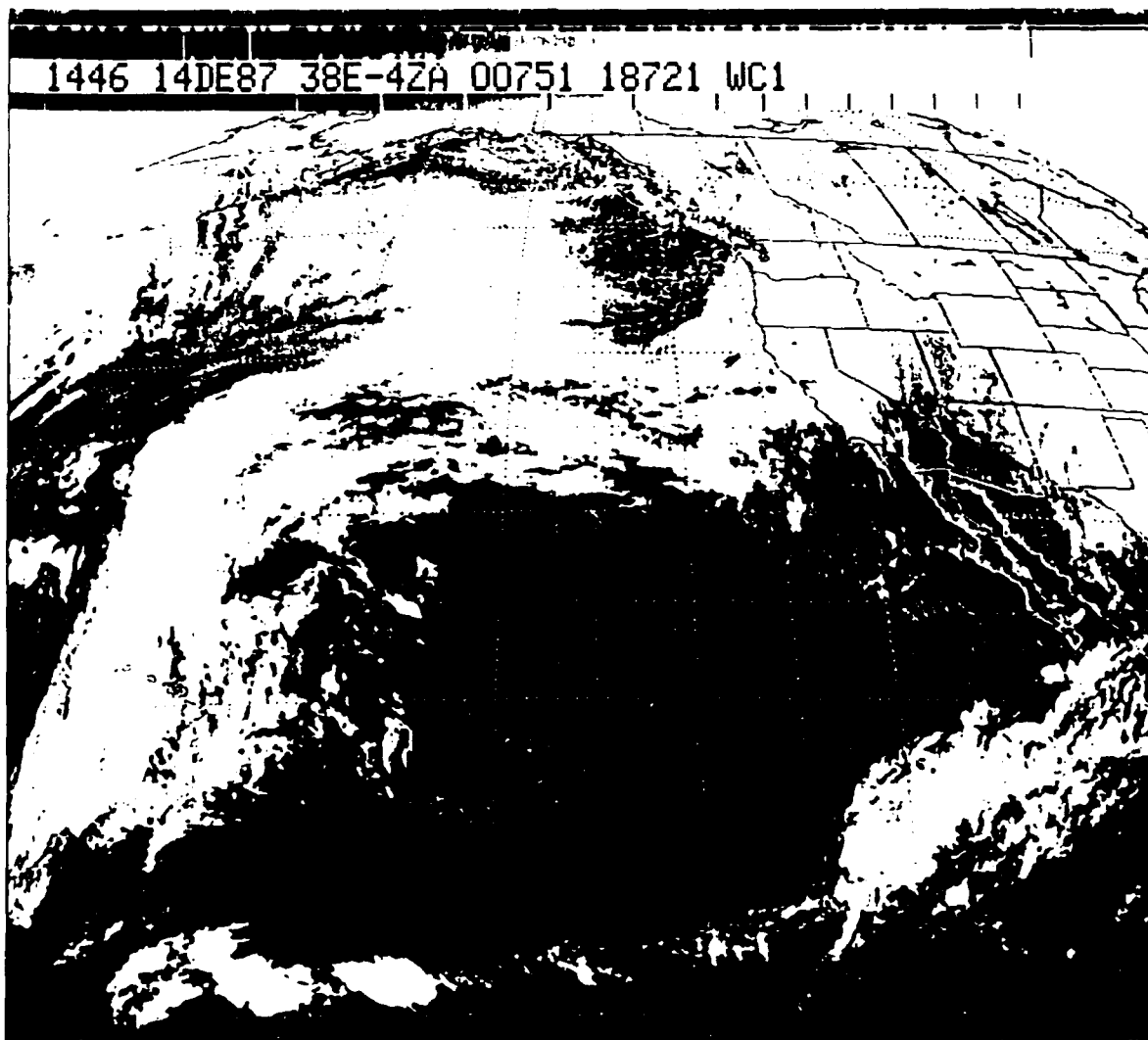Fig. 6   Geostationary Operation Environmental Satellite-WEST IR Sector for 1446 UTC 14 December 1987 Cyclone under study is at 37.5°N 148.0°W.
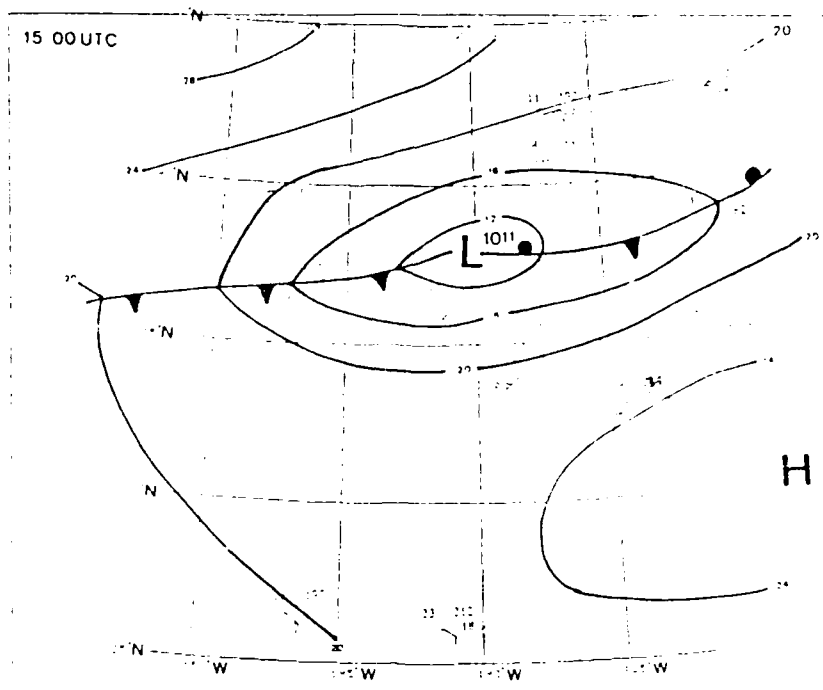
Fig. 7 Subjective Surface Analysis (mb) on 00 UTC 15 December 1987 Cyclone under study is at 37.5°N 141.0°W. The NMC objective analysis (Fig. 8) depicts the incipient cyclone with a closed 1016 mb isobar on the southern side of the baroclinic zone and agrees with the subjective analysis in Fig. 7. The western North Pacific Ocean cyclone, located at 53.0°N, 174.0°E, deepens 26 mb in 12 h to a central pressure of 946 mb.

The 500 mb NMC analysis (Fig. 9) shows the short-wave trough weaker with movement east to a position along 150.0°W. The vorticity pattern shows the CVC located near 46.0°N, 152.0°W has decreased in size and intensity and lags at a considerable distance to the northwest of the developing low near 37.5°N, 140.0°W. It is likely that this weakening may be an artifact attributable to the difficulties in oceanic analysis since no

Fig. 8   As in Fig. 3, except 00 UTC 15 December 1987
Cyclone under study is at 37.5°N 141.0°W.
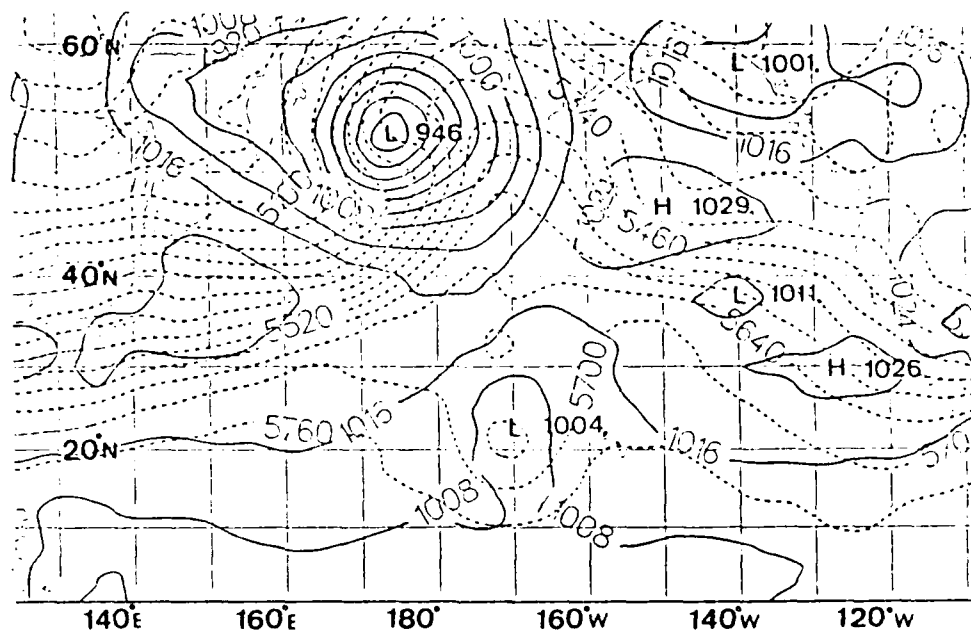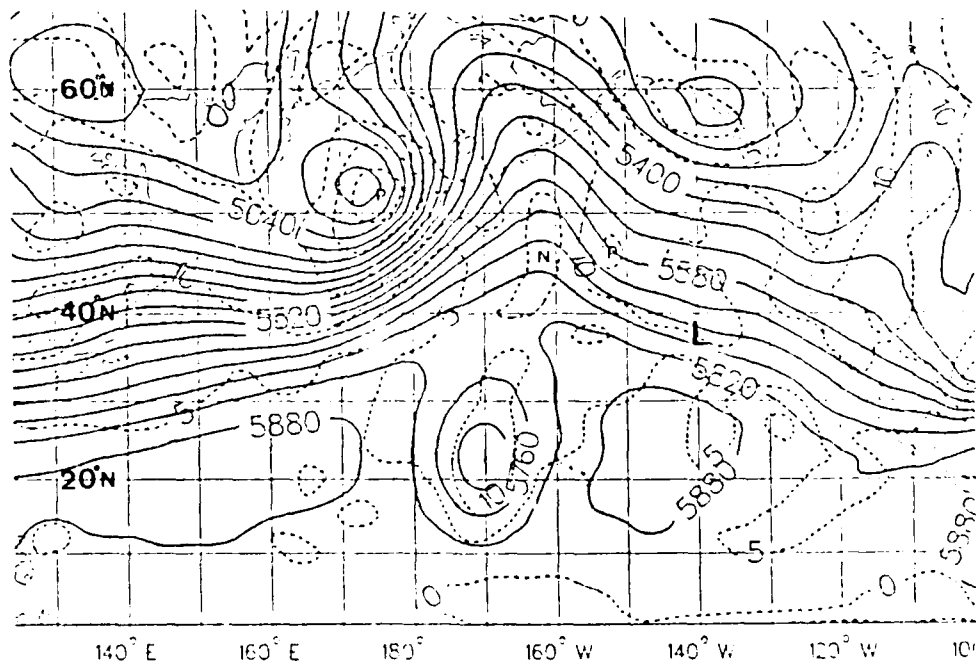

Fig. 9   As in Fig. 4, except 00 UTC 15 December 1987
Cyclone under study is at 37.5°N 141.0°W.

weakening is evident in the satellite imagery.   This short-wave

trough is now phasing with a long-wave trough which extends

18

southward from a vortex near 59.0°N, 137.0°W. At the same time, the long-wave ridge at 165.0°W is building in response to the strong upstream cyclogenesis and favors southward cold air movement into the Gulf of Alaska. The CVC associated with the western North Pacific Ocean cyclone strengthens and there is a strong cyclonic vorticity advection (CVA) area ahead of that storm.

The 250 mb analysis (Fig. 10) shows similar structure to the last time period with the jet streaks over the mid-latitude eastern and western North Pacific Ocean. However, a 50 ms^{-1} jet streak dramatically appears over western Alaska in response to the intensification of the central Pacific Ocean long-wave ridge. The developing low now is located under the eastern Pacific Ocean jet streak. However, if one argues that the 500 mb trough near 150.0°W is analyzed too weak, then this error would be also reflected in the 250 mb analysis. As a result, it is suggested that the surface cyclone may actually be positioned in the more favorable divergent side of the jet streak. This would enhance the rapid surface cyclogenesis at an earlier period than would otherwise be indicated by the objective analyses.

GOES IR imagery at 0046 UTC 15 December (Fig. 11) detects an emerging solid cloud area or cloud head near 40.0°N, 135.0°W which is well to the northeast of the surface analyses of the developing low. Bottger, et al. (1975) defines a head cloud in an explosively developing cyclone as a massive stratiform cloud area which appears elongated in a north-south direction due to an

anticyclonically curved cirrostratus shield which extends 500 km
to the north and east of the developing low. Cloud signatures
for normal developing waves do not posses this anticyclonic cloud
shield. Subsidence behind this cloud mass is sharply defined and
coincides with the axis of the 500 mb short-wave trough near
140.0^{O}W. This stengthening feature provides more evidence of the
poor 500 mb analysis in Fig. 9. The utilization of infrared (IR)
water vapor channel data (not shown) further enhances this
feature by filtering extreme low and high level clouds. This dry
zone is similar to that described by Bottger, et al. (1975) and
Kuo and Reed (1988) and usually signals the onset of explosive
cyclogenesis.
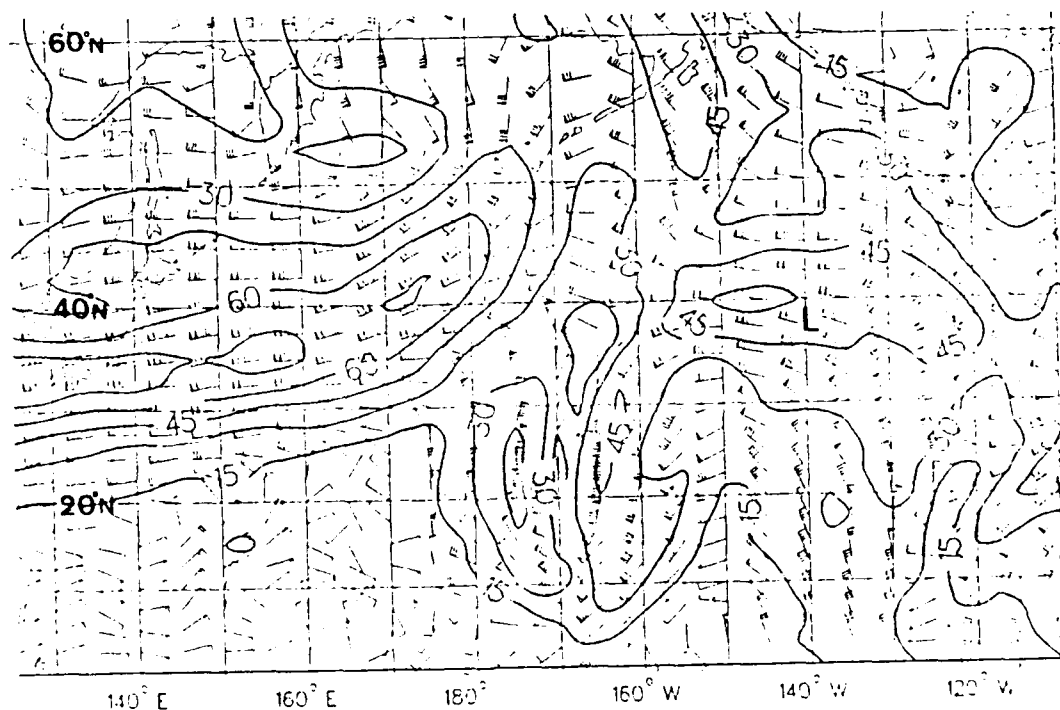
Fig. 10   As in Fig. 5, except 00 UTC 15 December 1987
Cyclone under study is at 37.5^{O}N 141.0^{O}W.
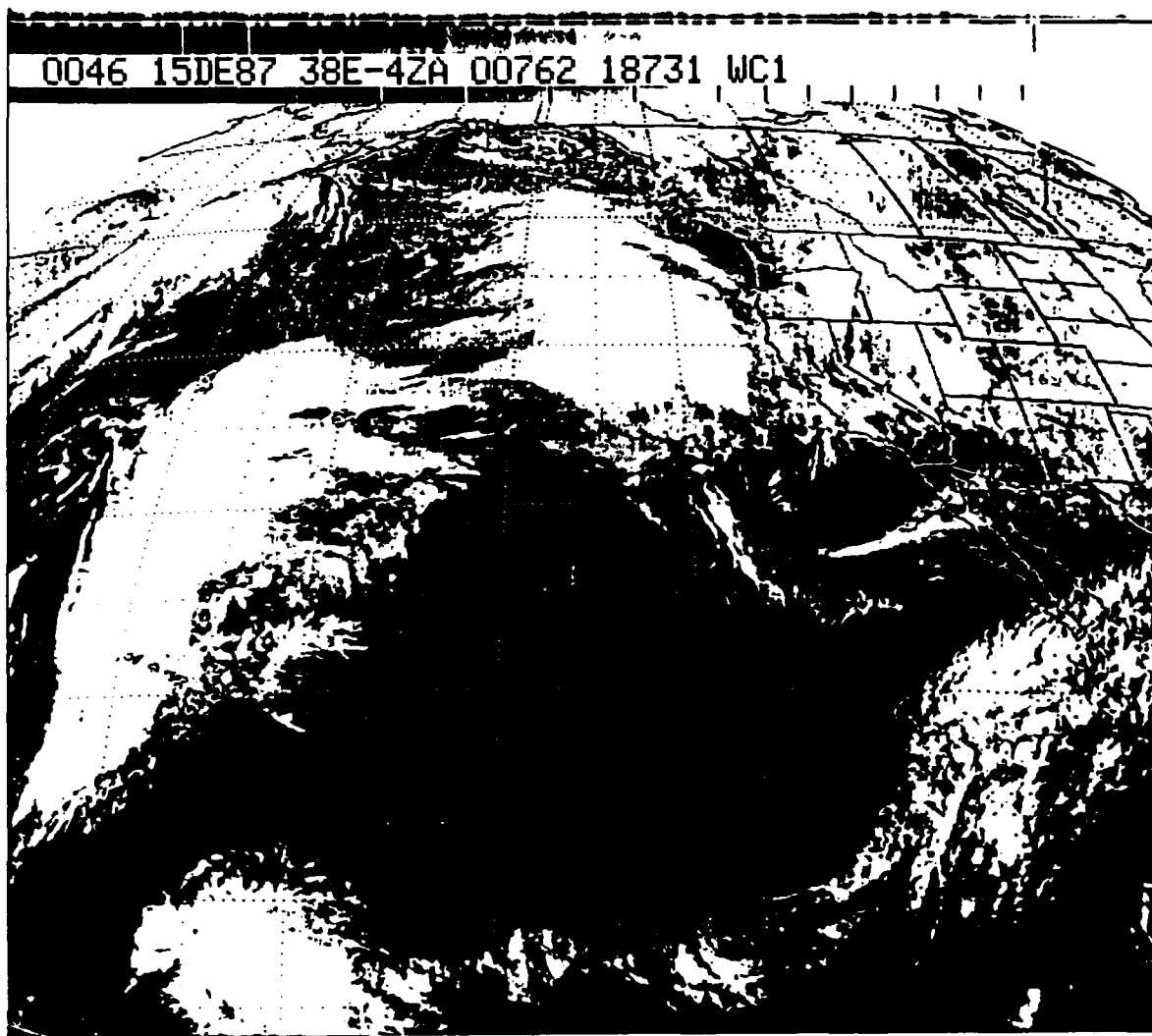
Fig. 11   As in Fig. 6, except 00 UTC 15 December 1987
Cyclone under study is at 37.5°W.

Six hours later, GOES (0546 UTC) imagery shows what appears

to be a dry slot formation near 39.0°N, 137.0°W (Fig. 12). The

position of the surface low remains to the southwest of the major

cloud mass and the dry region. The confidence of this position

of the cyclone is high as several ship reports indicate easterly
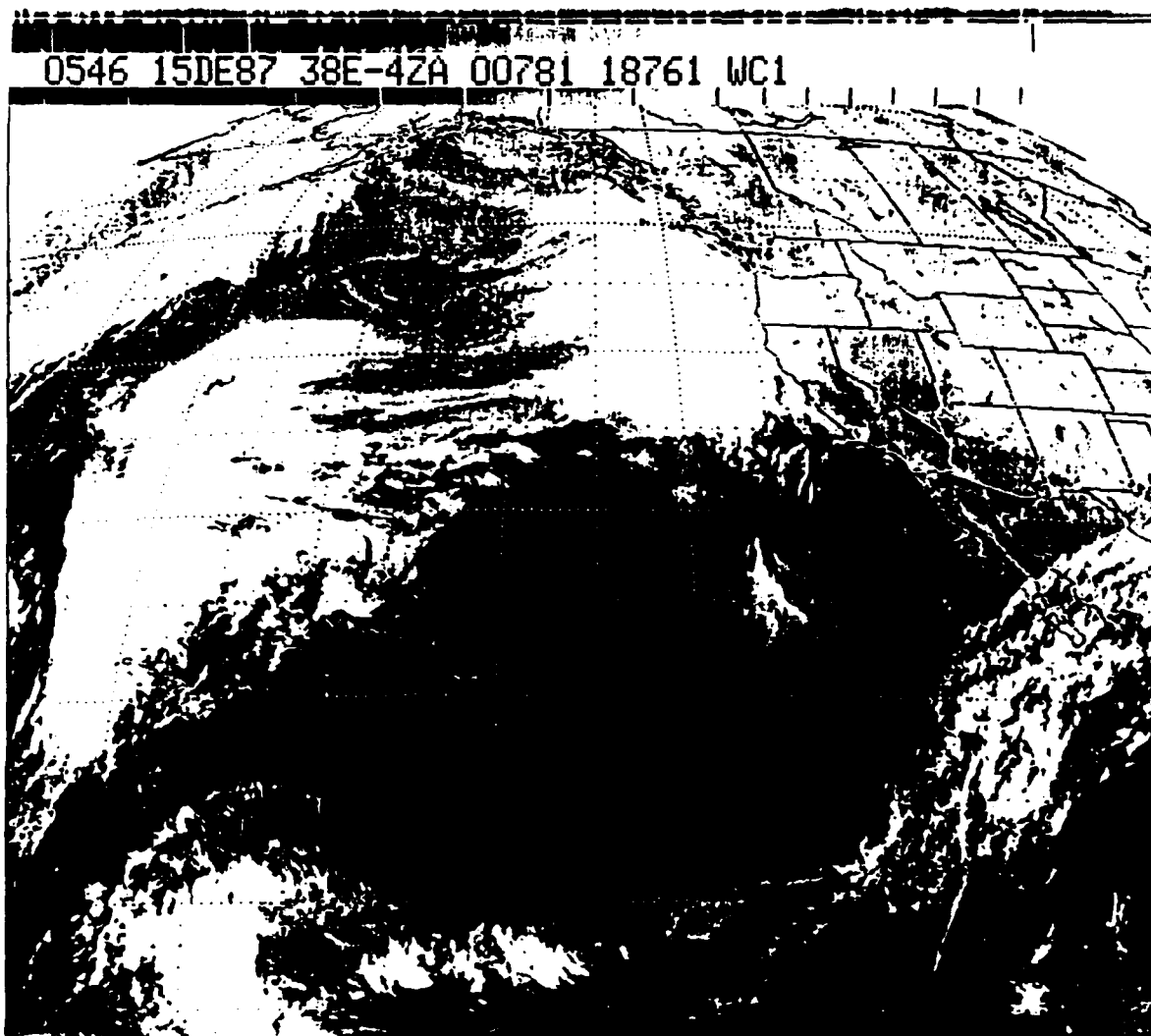
Fig. 12   As in Fig. 6, except 06 UTC 15 December 1987
Cyclone under study is at 37.5°N 137.0°W.

winds of 10-15 ms^{-1} just north of 40.0°N in the 00 UTC 15

December analysis.   Based on Junker and Haller (1980) satellite

classification, the center pressure expected would be close to

990 mb.   This large pressure difference (16 mb) between the

subjective analysis at 06 UTC (not shown) and cloud pattern

interpretation may be explained by the unique cloud pattern in

this case.   In their study, a composite of both forms of

cyclogenesis were included. In ordinary cyclones, a dry slot is formed later in its development as low-level cold descending dry air advects into the center of the cyclone from the northwest (Carlson, 1980). In cases where a developing short-wave with a strong subsidence overtakes the incipient low, the dry tongue will be better organized than with a typical cyclone. Consequently, the Junker and Haller estimate will indicate a system that is too intense.

At 12 UTC 15 December, subjective analysis (Fig. 13) indicates the cyclone is near 37.5°N, 133.8°W with a central pressure of 999 mb. This represents an 11 mb drop in pressure in 12 h and clearly indicates that the explosive phase is well under way. The NMC preliminary surface analysis (not shown) shows two cyclones, a 1006 mb low near 37.5°N, 134.0°W and a 1000 mb low near 40.0°N, 130.0°W. The latter low appears to be based on satellite imagery since there is no supporting surface data in this area. A ship, call sign (GBKE), located at 37.4°N, 129.2°W reports 1004.7 mb pressure and 10 ms^{-1} southwesterly wind which suggest that a broad area of low pressure extends northeast from the hand analysis position of the surface low to the center of
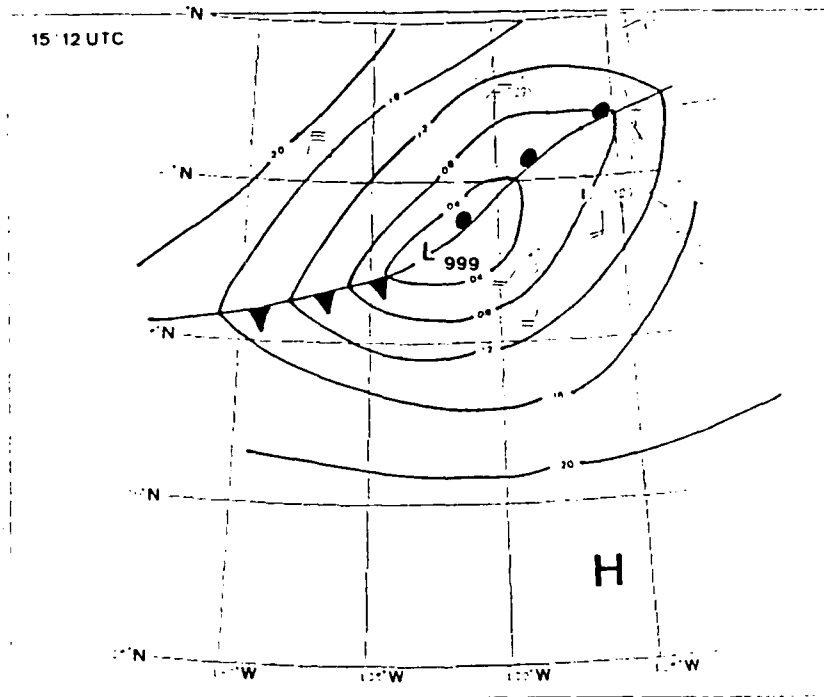
Fig. 13   As in Fig. 7, except 12 UTC 15 December 1987 Cyclone under study is at 37.5°N 133.8°W.

the well defined cloud mass near 40.0°N, 130.0°W. Pressure tendency falls exceeding 5 mb in 3 h result from the rapidly intensifying low. This assertion is supported by the ship (H9BQ) located at 36.0°N, 128.8°W, moving northeast in excess of 8 ms^{-1} with a -5.5 mb in 3 h pressure change.

The objective sea-level pressure (SLP) analysis (Fig. 14) compares well with the hand-drawn analysis. The objective analysis indicates a central pressure of 1003 mb. The thickness pattern shows a distinct thermal trough immediately west of the eastern Pacific Ocean cyclone with strong warm advection to the east of the cyclone center. The amplification of the upstream thermal pattern is now complete with a sharp ridge analyzed at 160.0°W. This observation of simultaneous reduction in the wavelength and increase in amplitude in the zonal flow just prior

to the onset of explosive cyclogenesis is consistent with finding of Mullen (1983). Examination of Fig. 8 and Fig. 14 demonstrates this phenomena.

The 500 mb analysis shows the upstream short-wave trough has strengthened and is immediately west of the surface system (Fig. 15). This deepening is due in part to the strong cold air advection west of the surface cyclone (Fig 14). Recall there is strong evidence that the 500 mb trough was analyzed too weak and too far west for the previous time periods. Therefore, it is

Fig. 14   As in Fig. 3, except 12 UTC 15 December 1987 Cyclone under study is at 37.5°N 133.8°W.
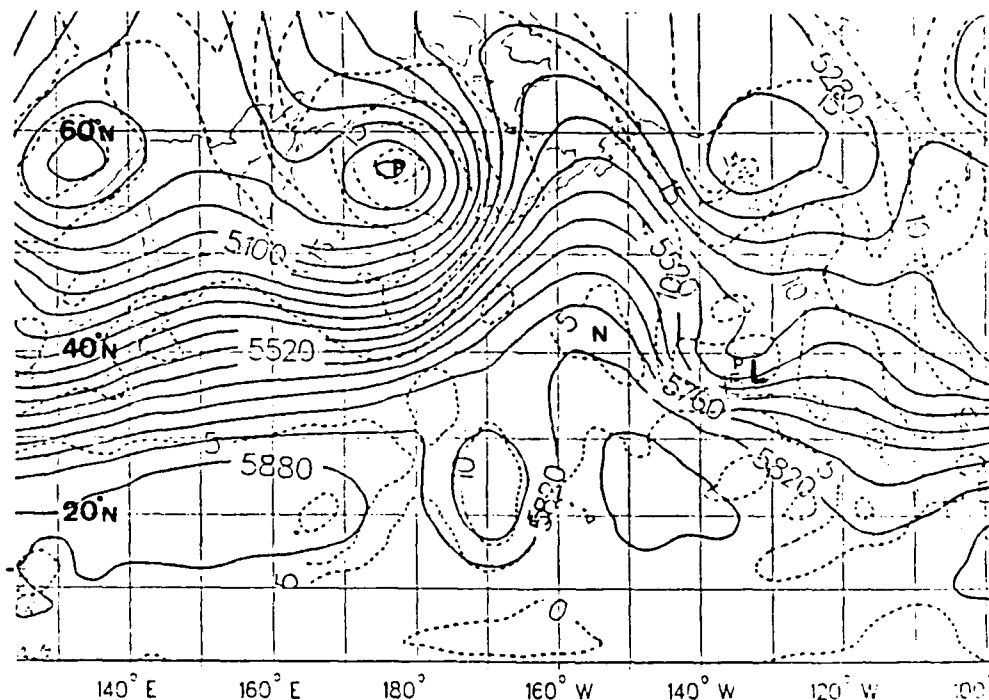
Fig. 15   As in Fig. 4, except 12 UTC 15 December 1987
Cyclone understudy is at 37.5°N 133.8°W.

difficult to know how much trough intensification occurred over
the past 24 h.   The maximum vorticity in the trough is 19 x 10⁻
$5s^{-1}$ and a classic CVA pattern is found over the surface cyclone
near 40.0°N, 135.0°W.   To the west, the amplifying upstream ridge
is found near 155.0°W.

The 250 mb analysis shows continued intensification of the
jet streak to the northwest of the surface low (on the east side
of the ridge) as it merges with the eastern North Pacific Ocean
jet streak (Fig. 16).   The axis of maximum 250 mb winds is now
south of the surface cyclone.   This jet streak pattern favors
strong upper level divergence over the surface cyclone.

GOES imagery shows that the cloud head has developed into a
definite comma cloud shape (Fig. 17).   The dry slot is also well
formed and a cloud band begins to hook around the center of the
cyclone. The Junker and Haller (1980) satellite classification

26

would indicate a central pressure of 980 to 989 mb, lower than these analyses indicate. This is about half the pressure interpretation error noted 12 h earlier. Dry air begins to overrun the frontal cloud band while the cloud mass has expanded over California. Open cell stratocumulus to the west of the cyclone indicate that a significant degree of cold air advection is occuring west of the cyclone.

During the next 12 h period, spectacular development is evident in the subjective analysis (Fig. 18). The central SLP steadily falls 21 mb during the 12 h period to its lowest value
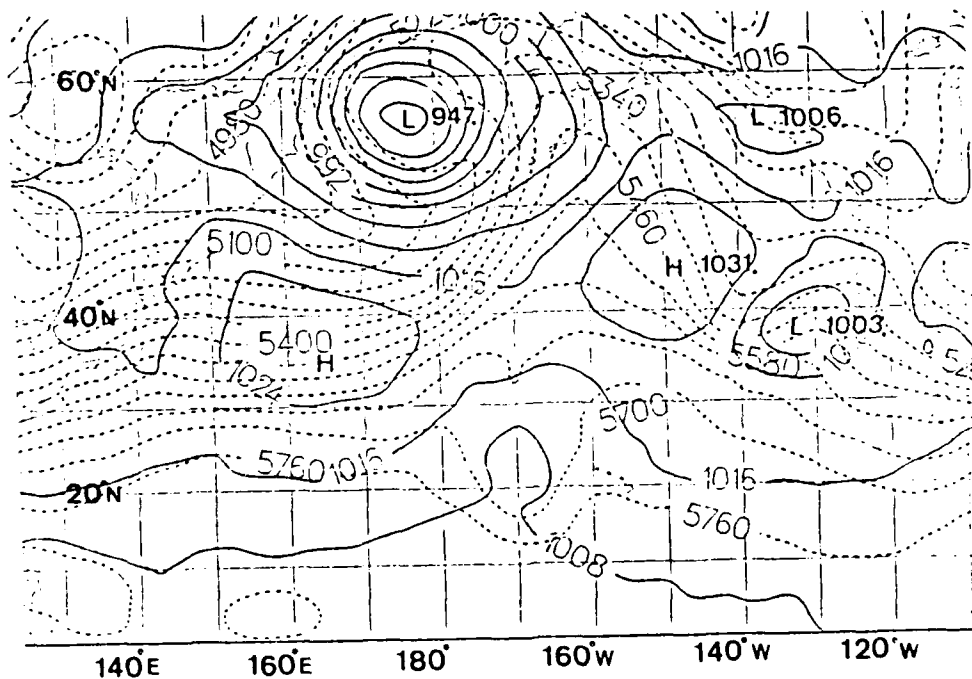

Fig. 16   As in Fig. 5, except 12 UTC 15 December 1987 Cyclone under study is at 37.5°N 133.8°W.
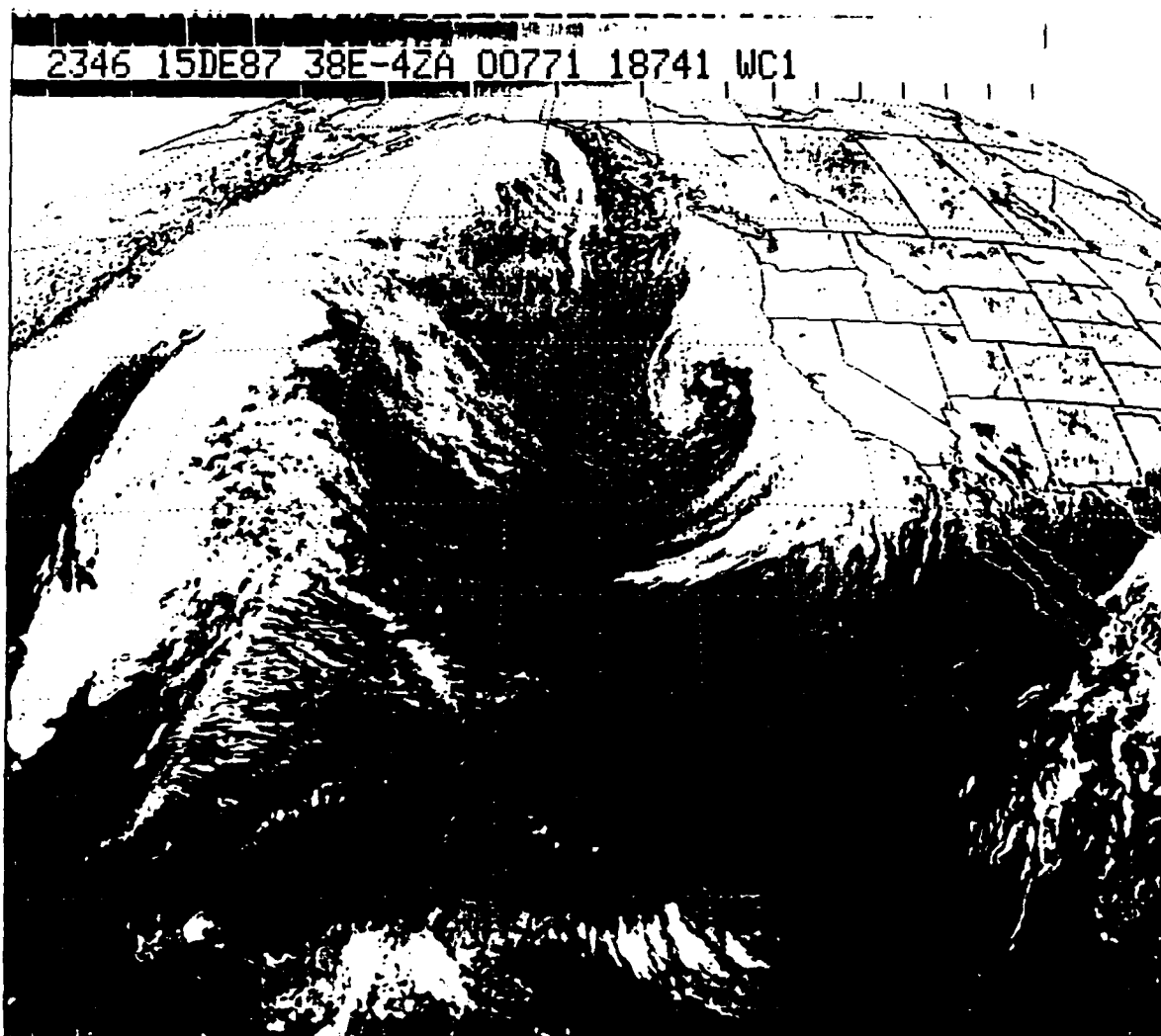
Fig. 17   As in Fig. 6, except 00 UTC 16 December 1987
Cyclone under study is at 37.5°N 127.8°W.

of 978 mb. This represents a 2.0 Bergeron event for the 24 h

period ending 00 UTC 16 December. At this time of maximum

intensity, the storm rapidly occludes. One report from a ship

(GBKE7) located 525 km northwest of the storm reports north

northwest winds at 33 ms^{-1} with a SLP of 996.9 mb. Another ship

(ELEK), 225 km west of the center, reports northwest winds at 26

ms^{-1} a SLP of 982.5 mb. In comparison, the 985 mb SLP on the NMC

surface grid point analysis (Fig. 19) is thought to reflect

limitations in the objective analysis and data availability. The distinct thermal trough is analyzed west of the mature storm with a thickness maximum centered over the low.

The 500 and 250 mb analyses (Fig. 20 and 21), as well as the satellite imagery (Fig. 22), show the cyclone is nearly occluded by 00 UTC 16 December. The intense $22 \times 10^{-5}s^{-1}$ CVC and upper level vortex associated with the cyclogenesis is aligned vertically over the surface low. The 500 mb long-wave ridge is now located along $150.0^{\circ}W$ (Fig. 20). The 250 mb wind flow shows a sharp trough line vertical over the 500 mb system. A jet streak, maximum of 70 ms^{-1}, is now oriented north-south, west of the surface low (Fig. 21).

Cold open cell stratocumulus begin to advect into the center of the low from the northwest (Fig. 22). The dry slot and curved cloud band associated with the occluded front is very well defined. Rain showers have moved inland over California. The Junker and Haller (1980) classification indicate that this well defined cyclone lies within the 970 to 979 mb SLP range.

During the anti-climatic final two phases, the system drifts southeast 5 ms^{-1} but generates destructive seas and surf along southern California coastal waters (Storm Data (National Oceanic and Atmospheric Administration, 1987)). The cyclone remains vertically aligned and its movement is steered by the upper level low (not shown). The storm's pressure remains constant from 00
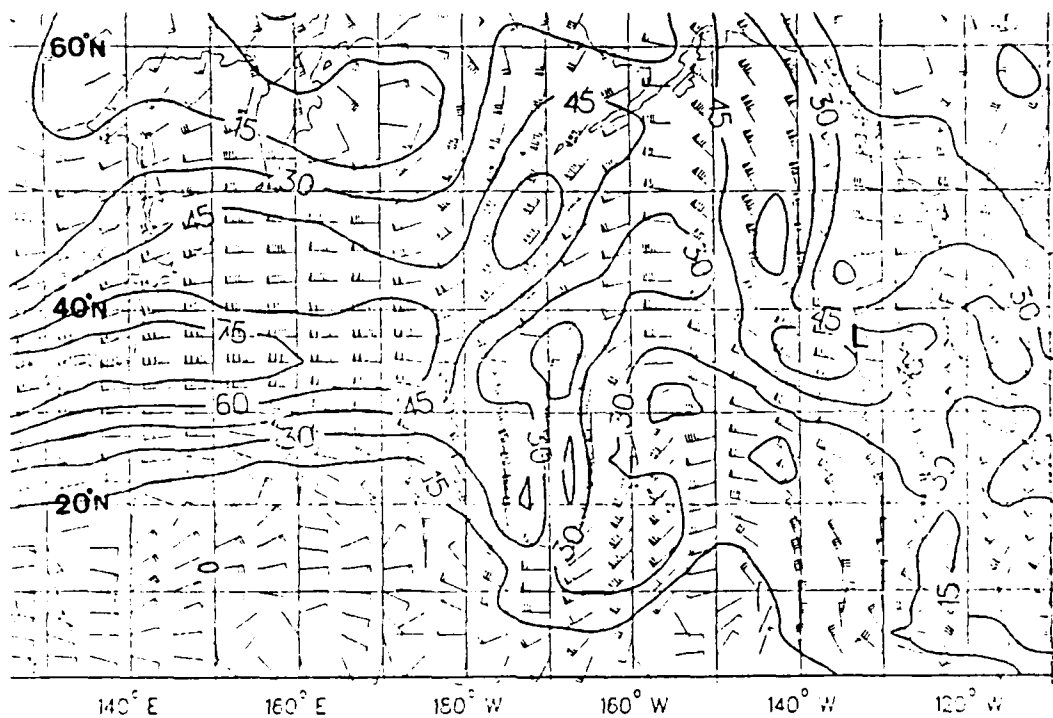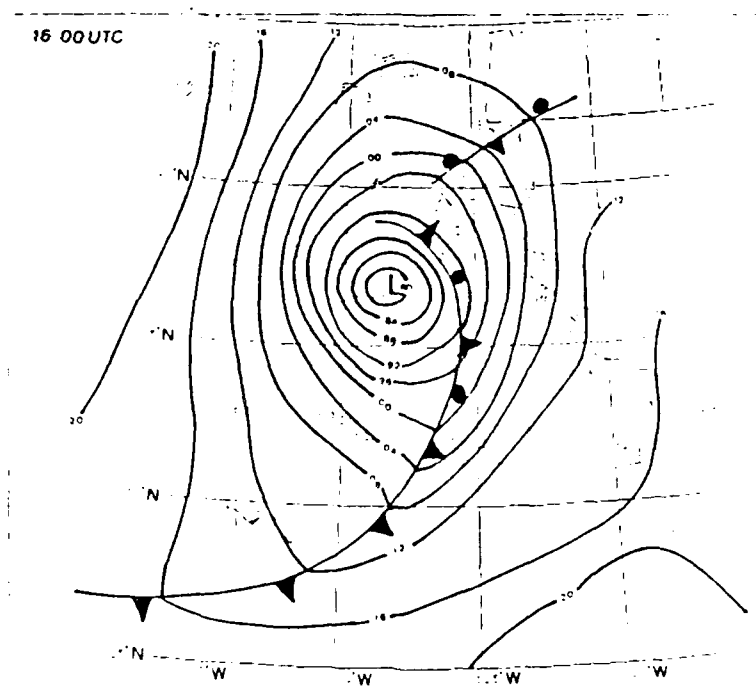
Fig. 18   As in Fig. 7, except 12 UTC 15 December 1987
Cyclone under study is at 37.5°N 133.8°W.
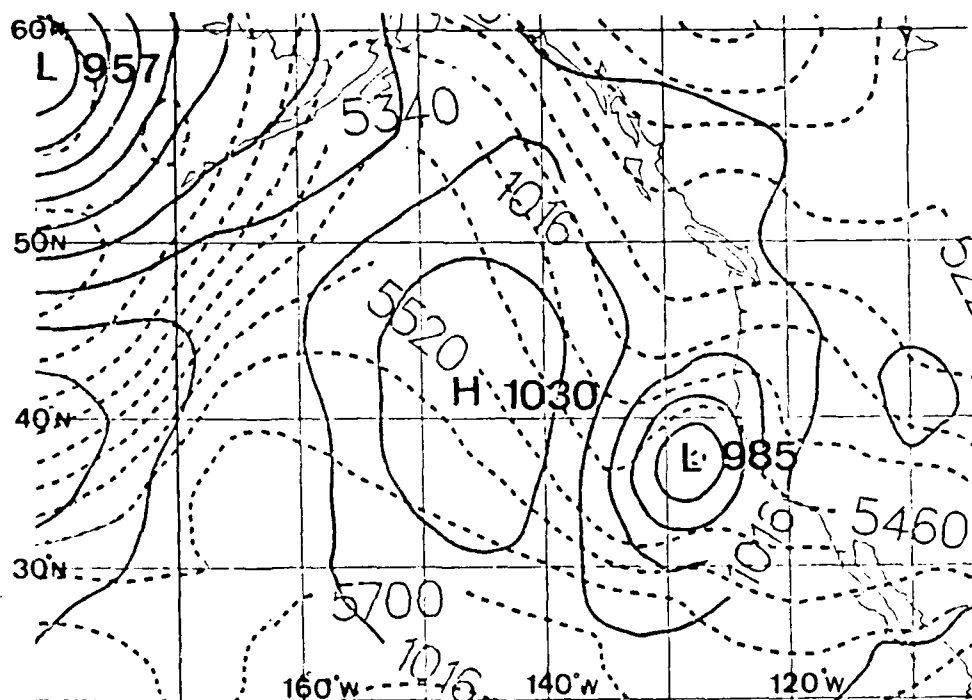
Fig. 19   As in Fig. 3, except 00 UTC 16 December 1987
Cyclone under study is at 37.5°N 127.8°W.
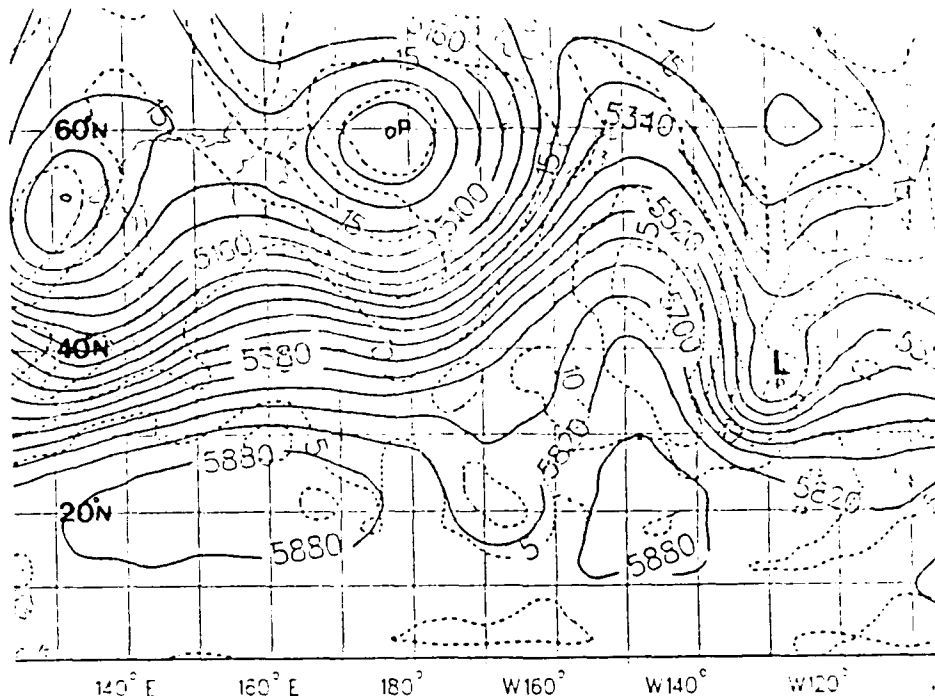
Fig. 20   As in Fig. 4, except 00 UTC 16 December 1987
Cyclone under study is at 37.5°N 127.8°W.
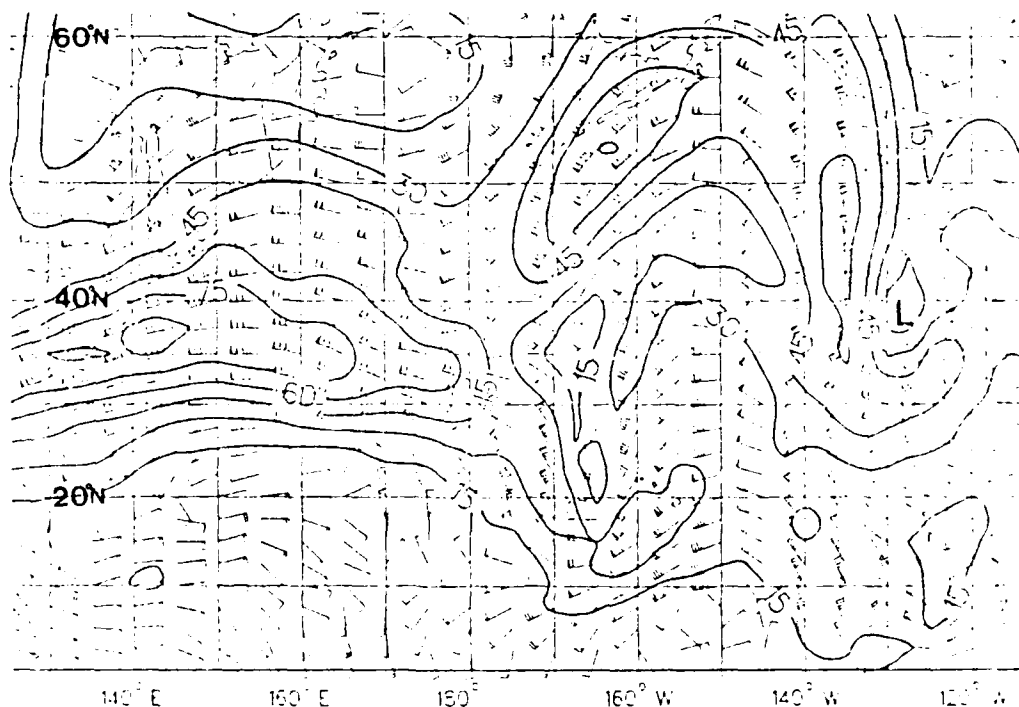
Fig. 21   As in Fig. 5, except 00 UTC 16 December 1987
Cyclone under study is at 37.5°N 127.8°W.
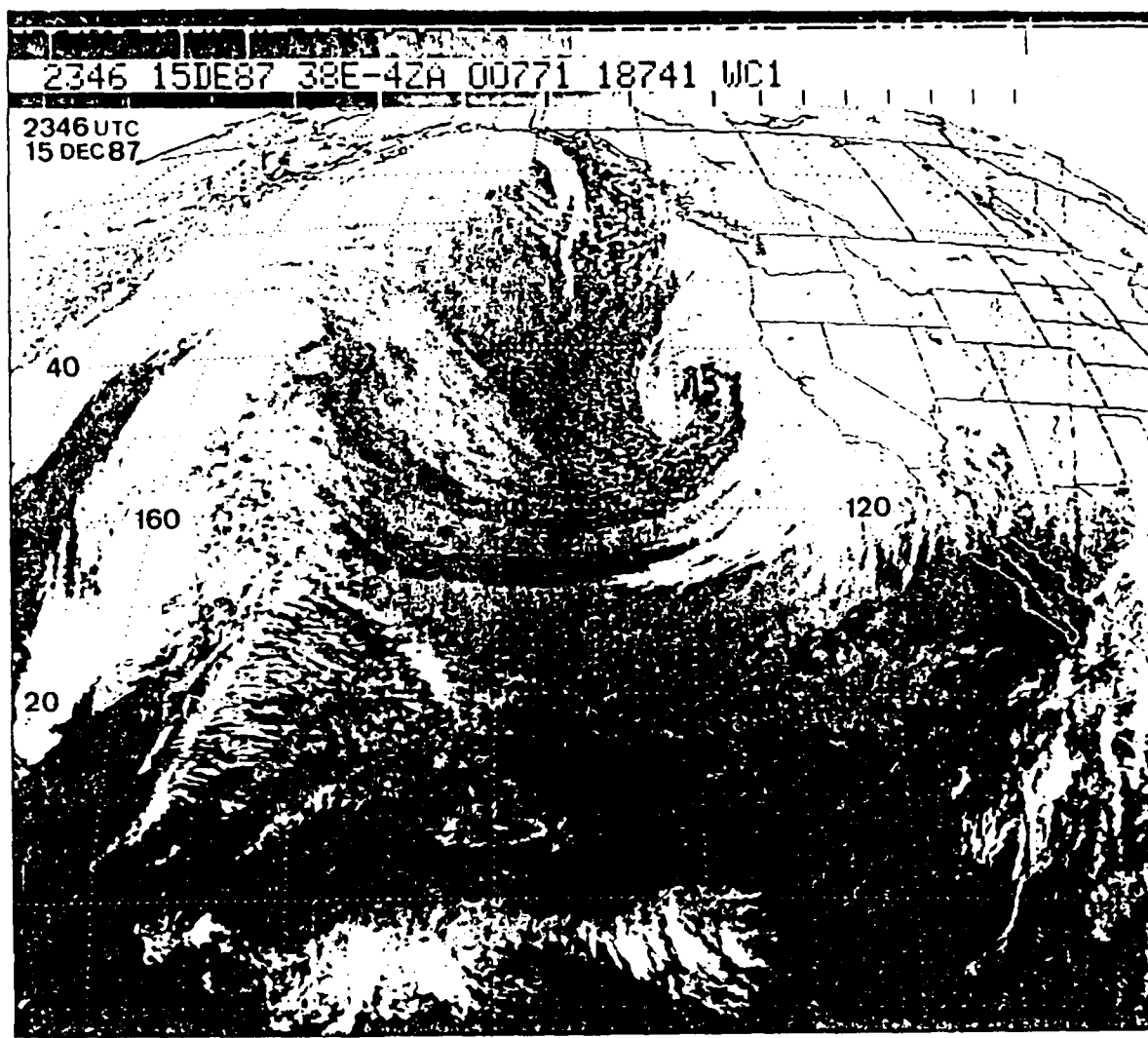
Fig. 22   As in Fig. 6, except 00 UTC 16 December 1987
Cyclone under study is at 37.5°N 127.8°W.

UTC to 12 UTC 16 December as the vortex aloft deepens slightly.

The 500 mb CVC reaches its maximum intensity of 24 x $10^{-5}s^{-1}$ and

is located in the center of the storm (slight cyclonic advection

during the past 12 h). By 12 UTC 16 December, the 1000-500 mb

thermal trough weakens and the 250 mb jet streak narrows and

remains nearly stationary to the west of the storm.

B. Verification of NGM and NOGAPS "Operational" Model Forecasts

The accuracy of two operational NWP models in forecasting this event are evaluated in this section. They are the NMC Nested Grid Mesh (NGM) and the FNOC Navy Operational Global Atmospheric Prediction System (NOGAPS 3.0) model surface prognostic charts.

For the mariner, a short range (6-12 h) but highly accurate forecast does not satisfy the operational and safety requirements over the open ocean. For the slower transiting vessels, ideally a longer range (36-72 h) forecast which can provide optimal ship routing guidance becomes a necessity. While the global model forecasts provide generally good guidance for the planetary wave structure, often the synoptic scale explosive cyclogenesis event is not resolved. The general storm track area may be known with sufficient accuracy during a one week period but the questions as to when a storm will actually form and how intense it will actually become are problems which still plague weather forecasters and mariners.

Table 3 shows that the NGM exhibited significant error for the 36-h forecasts during the explosive period. Specifically, the 00 UTC 16 December forecast initialized 12 UTC 14 December was 22 mb too weak and the cyclone was displaced 400 km southeast of the actual position. The forecast track error of 600 km at 00 UTC 17 December (based on 12 UTC 15 December fields) is probably due to an erroneous estimate that the eastward moving cloud head northeast of the developing surface low possesses a

33

substantial amount of cyclonic vorticity (not shown). The subsequent forecast track of the low tended to follow this CVC to a position near Reno, Nevada. These errors are consistent with initial NMC analyses being too zonal. The model then moves the developing low too far east while not deepening it enough.

TABLE 3
NESTED GRID MESH (NGM) 36-H FORECAST SKILL

36-H FORECAST VT (UTC)	1500	1512	1600	1612	1700	1712
MIN SLP (MB)	1015	N/A	1000	992	988	998
SLP ERROR (MB)	+4	N/A	+22	+12	-4	-4
POSITION ERROR (KM)	200	N/A	400	400	600	150

The errors in the cyclone intensity and location from a 72 h NOGAPS 3.0 forecast are summarized in Table 4. The 20 mb underdevelopment and 320 km slow track (west of the verifying position) is also attributed to faulty initialization. The only initial difference between the FNOC surface analysis (Fig. 23) and the NMC surface grid point analysis (Fig. 3) is that the FNOC's depiction of the cyclone near $170.0^{\circ}E$ appears to be 5 mb higher. Aloft, the 250 mb jet maximum just east of Kamchatka is 20 ms^{-1} weaker in the FNOC analysis (Fig. 24) than in the NMC 250 mb analysis (Fig. 5). The NOGAPS forecast at TAU 24 (Fig. 25) under forecasts the dateline cyclone by 11 mb and weakens the thickness trough and ridge associated with the eastern Pacific Ocean explosive low as compared to Fig. 14. Consequently, a

chain of events is suggested which builds the mid-Pacific Ocean upper level ridge and deepens the eastern Pacific Ocean long-wave trough at a slower rate in the forecast series than was actually observed. This may explain why the NOGAPS 24 h forecast 250 mb jet streak over the Gulf of Alaska (Fig. 26) is 20 ms^{-1} weaker than analyzed by NMC (Fig. 16). The improved forecast positionafter 12 UTC 16 December may be explained by the storm's slowed movement as it becomes vertically aligned. The NOGAPS forecast provided excellent long-wave positional and thickness pattern accuracy throughout its forecast run but lacked the proper intensity in these features. Future studies are encouraged to investigate numerical model sensitivity to slight variations in initial analyses fields.

TABLE 4
NAVY OPERATIONAL GLOBAL ATMOSPHERIC PREDICTION
SYSTEM (NOGAPS) FORECAST SKILL INITIALIZED
12 UTC 14 DECEMBER 1987

FORECAST VT (UTC)	1500	1512	1600	1612	1700	1712
MIN SLP (MB)	1013	1007	998	994	997	1001
SLP ERROR (MB)	+2	+8	+20	+14	+5	-1
POSITION ERROR (KM)	390	430	320	290	190	140
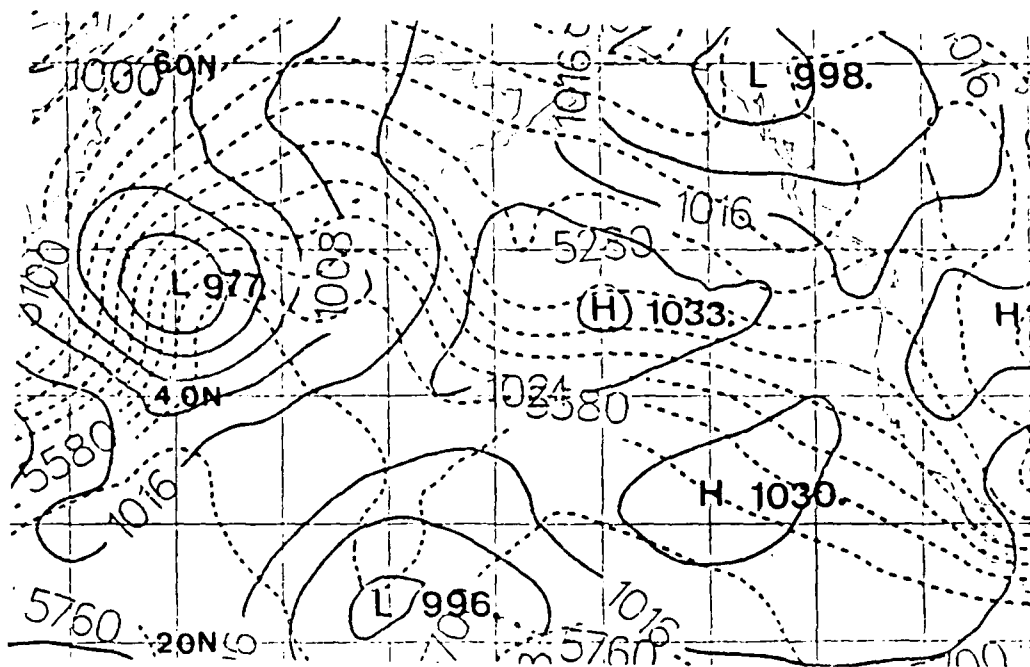
Fig. 23   As in Fig. 3, except NOGAPS Analysis 12 UTC
14 December 1987 Cyclone under study is at 37.5°N
148.5°W.
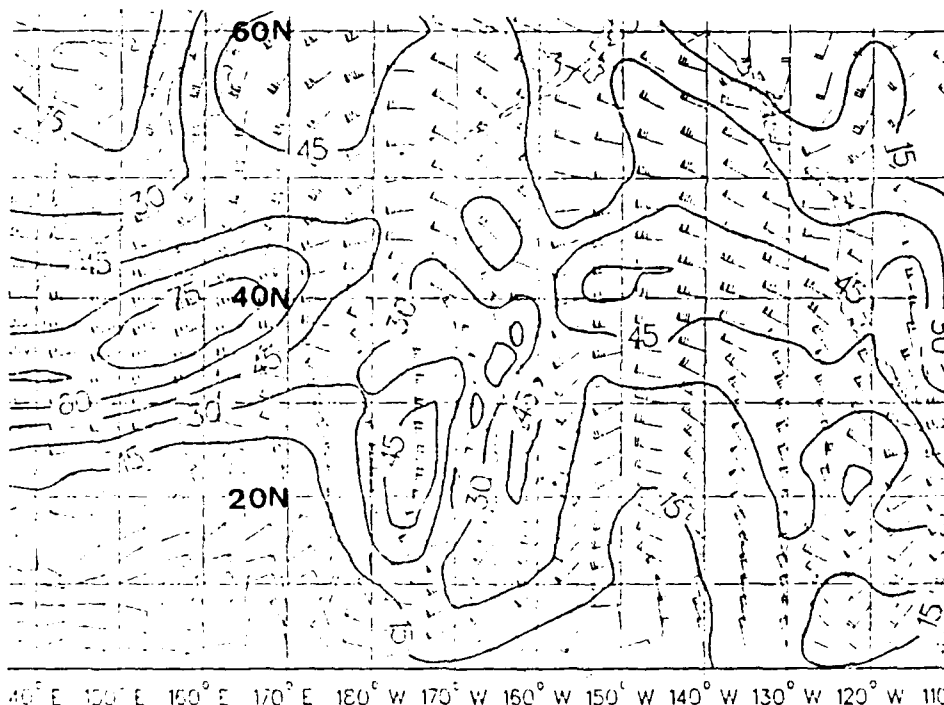
Fig. 24   As in Fig. 5, except NOGAPS Analysis 12 UTC
14 December 1987 Cyclone under study is at 37.5°N
148.5°W.
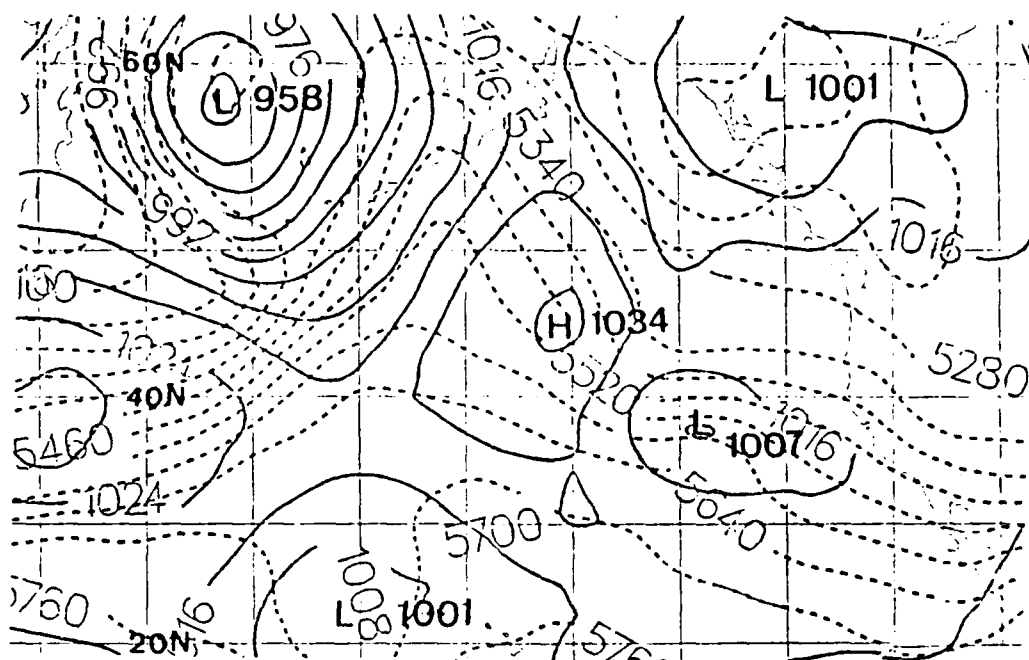
Fig. 25   As in Fig. 14, except NOGAPS 24 h Forecast VT
12 UTC 15 December 1987 Cyclone under study is at
37.5°N 133.8°W.
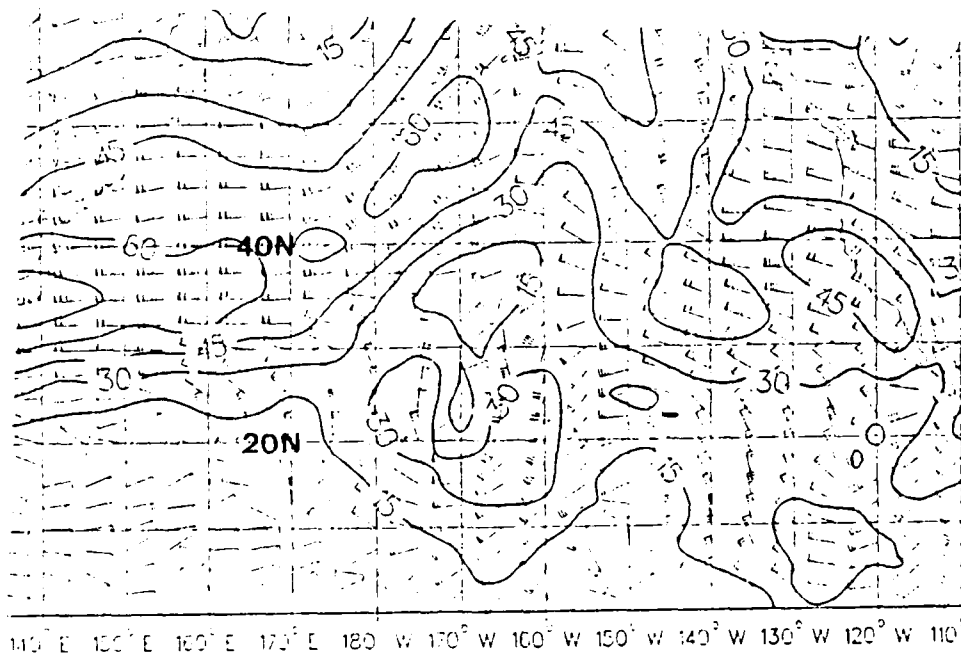
Fig. 26   As in Fig. 16, except NOGAPS 24 h Forecast
VT 12 UTC 15 December 1987 Cyclone under study is at
37.5°N 133.8°W.

III. BUDGET ANALYSIS

A. Budget introduction

In this section, the mass and vorticity budget analysis using the quasi-Lagrangian diagnostic techniques is used to determine the transport of storm properties relative to the moving cyclone center over the eastern Pacific Ocean during the period 14-17 December 1987. Statistics for the 6° radius budget volume will be reported here as it best represents the cyclone circulation for this case. Significant differences between the 6° volume and the 4° and 8° volumes will be addressed as appropriate. Comparisons to Calland (1983) and Cook (1983) cyclone case studies will also be discussed. The mass budget analysis quantitatively describes the static stability and horizontal and vertical mass transport for the storm. The budget equation for mass is

$$\frac{dM}{dt} = LT + VT,$$

(3.1)

where the mass is

$$M = \int_{1000\ mb}^{100\ mb}\int_{0}^{\beta_B} \int_0^{2\pi} \frac{1}{g}\, r^2 \sin\beta d\alpha d\beta dp,$$

(3.2)

the lateral transport is

$$LT = - \int_{1000\ mb}^{100\ mb}\int_0^{2\pi} \frac{1}{g}\, (\vec{U} - \vec{W}_0)_\beta r \sin\beta_B d\alpha dp\, |_{\beta_B}$$

(3.3)

and the vertical transport is

$$VT = -\int_0^{\beta_B}\int_0^{2\pi} \frac{1}{g}(\omega - \omega_B)r^2 \sin\beta\,d\alpha\,d\beta\,|_p. \qquad (3.4)$$

Vertical velocities are computed kinematically and interpolated to the budget volume. On the other hand, the vorticity budget equation (Eq. 3.5) and its terms as defined in Table 5, account for the sources and sinks and transport of absolute vorticity during cyclone development.

$$\frac{\overline{\delta\zeta_a}}{\delta t} = -\vec{\nabla}\cdot(\vec{V}\zeta_a) - \frac{\partial}{\partial p}(\omega\zeta_a) - \zeta_a\vec{\nabla}\cdot\vec{V} + \vec{k}\cdot\vec{\nabla}\omega\times\frac{\partial\vec{V}}{\partial p} + \vec{F} + \vec{R}$$

$$(3.5)$$

The source and sink magnitudes reflect typical values found in other budget studies.

Table 5. BUDGET TERMS IN THE VORTICITY EQUATION

Term #	Term	Source or Sink
1	$-\vec{\nabla}\cdot(\vec{V}\zeta_a)$ lateral transport	strong source
2	$-\frac{\partial}{\partial p}(\omega\zeta_a)$ vertical flux	weak or moderate sink
3	$-\zeta_a\vec{\nabla}\cdot\vec{V}$ divergence	strong source
4	$+\vec{k}\cdot\vec{\nabla}\omega\times\frac{\partial\vec{V}}{\partial p}$ tilting	weak or moderate sink
5	$+\vec{F}$ frictional dissipation	weak or moderate sink
6	$+\vec{R}$ residual	weak or moderate sink or source

From the integration of the flux form of the vorticity equation, the absolute vorticity time tendency $\delta\zeta_a|\delta t$ is equal to the terms in Table 5. The vorticity equation can be visualized as the summation of transport terms (#1 and #2) and source and sink terms (#3-#6). Total horizontal transport (term #1) can be

39

partitioned into mean and eddy modes. The mean mode represents the vorticity transport due to mean lateral convergence/divergence of the cyclone. Jet streaks, CVA and upper level short-wave troughs are important mechanisms that contribute to the eddy mode component. The vertical flux (term #2) can also be separated into a mean and eddy mode and serves to vertically redistribute the vorticity brought into the budget volume from lateral transport.

The vorticity divergence term (term #3) represents a source when flow is convergent and sink when divergent. It contributes to ς_a during cyclonic development and then to a lesser extent as a cyclone dissipates. Tilting (term #4) usually acts as a sink while friction (term #5) is always considered a sink. The friction term is estimated using the bulk aerodynamic method following Calland (1983). The residual (term #6) contains the accumulation of errors due in part to finite differencing and interpolation, observational errors in the final data fields and to the inherent estimates that occur when kinematically deriving vertical velocity fields. The residual term can be a source or a sink but must be of a small magnitude if one is to have confidence in the overall budget results.

B. Mass Budget Analysis

Static stability trends for the translating cyclone budget volume are monitored using a static stability index (SI) based on the hydrostatically computed area-averaged potential temperatures. The differences between storm volume potential

temperatures at 500 mb and 1000 mb is computed and is presented
in units of degrees K per hundred millibars (Fig. 27). The SI
shows a destabilization trend during the 48 h period of storm
development. The greatest SI fall (1.6°K per 100 mb) in 12 h
occurs from 00-12 UTC 15 December and coincides with the
beginning of rapid development. The SI continues to fall until
12 UTC 16 December with an additional 0.3° K/100 mb drop. The SI
values for radius 4° and 8° show similar tendencies, and 4°
budget volume shows slightly weaker stability than the 6° and 8°
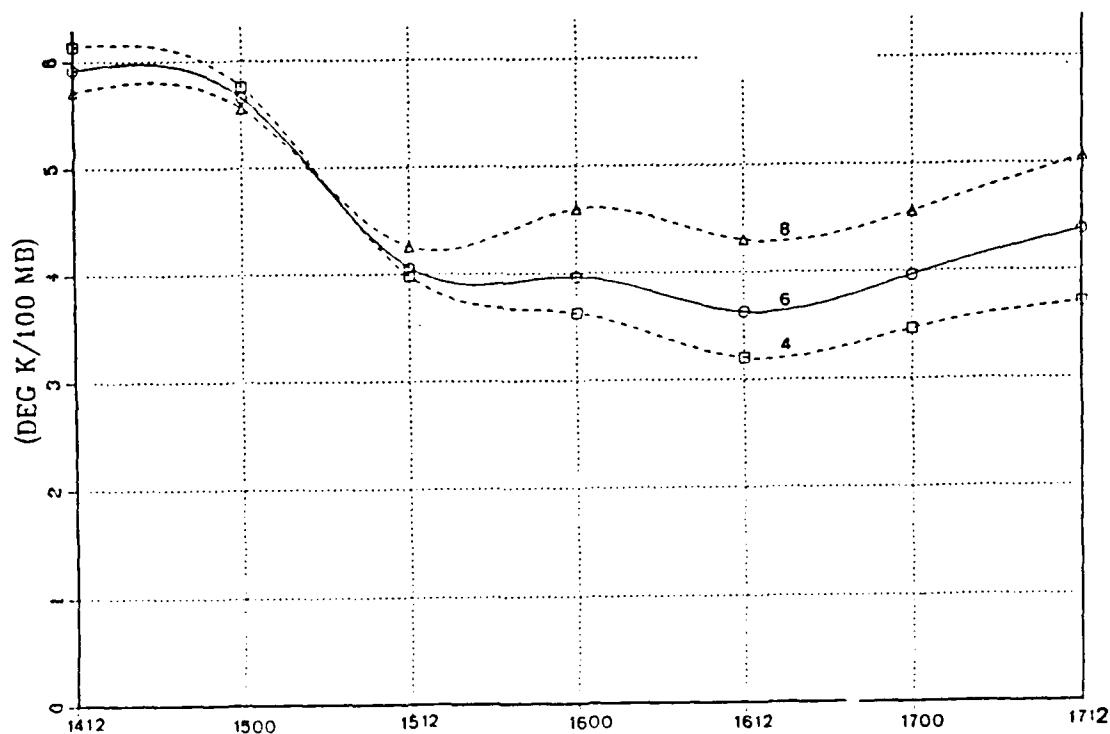
Fig. 27 Static Stability index: Values of anlayzed
data for a 4, 6 and 8 deg radius budget volume centered
on the eastern North Pacific Ocean cyclone. Values in
°K/100 mb. Time 1412 refers to 1200 UTC 14 December
1987.

41

budget volumes. After the cyclone occludes, a general stabilization in the lower half of the troposphere occurs with SI increasing slightly. A similar SI tendency was observed for Calland's northeast Pacific Ocean mid-latitude explosive event at a 6° budget volume. A northeast Atlantic Ocean polar low explosive event studied by Cook using a 4° budget volume also showed the SI decreasing throughout the cyclone's life and eventually becoming conditionally unstable as the cyclone reached maximum intensity.

Time sections of the budget volume area-averaged potential temperature show the temperature changes responsible for changing the lapse rate (Fig. 28a). Pronounced cooling in the mid-troposphere is evident during the period 00 to 12 UTC 15 December and is primarily responsible for the lapse rate decreases. The 1000 mb potential temperature shows little change during this period. Above 225 mb, the budget volume warms slightly until the occlusion process is well underway (12 UTC 16 December). Calland showed initial warming in the lowest and highest layers in the troposphere with little change in the mid-troposphere. As that Pacific Ocean cyclone intensified, the entire budget volume cooled. Cook's analysis of a polar low showed cooling in the lower half of the troposphere during the development stage of the cyclone. After 24 h, warming in the lower troposphere helped to further destabilize the cyclone.

The mass budget equation (Eq. 3.1) relates the mass time tendency to the sum of the lateral (horizontal) transport (flux)

and vertical transport (flux) terms. The horizontal mass transport (Fig. 28b) is a measure of the horizontal convergence/divergence patterns and the level of non divergence (LND) for the cyclone. As would be expected with a developing cyclone, strong low-level inflow associated with surface layer convergence and middle and upper level outflow associated with divergence dominates. What is unexpected with this storm is the initially well established transport pattern at 12 UTC 14 December. This initial pattern shows distinct outflow above 400 mb with inflow below, even when the surface cyclone is in the weak frontal wave ridge. The LND which begins at 400 mb, lowers dramatically to 730 mb during the first 24 h and to 800 mb during the second 24 h of the cyclone's life.

The continued lowering of the LND well after the mature phase is different in structure compared to the Calland and Cook cases. Calland showed a LND which oscillated between 625 and 500 mb until maximum cyclogenesis and then gradually reduced in height during the storm's dissipation. Cook showed the LND rising throughout most of his cyclone's life (600-450 mb). In both cases, maximum low-level convergence and upper level divergence coincided closely with the period of maximum cyclone intensity. In this case the strongest inflow occurs at 925 mb just prior to the cyclone reaching maximum intensity (18 UTC 15 December) and is more than four times the maximum outflow at any one level. The transport in the entire column of the
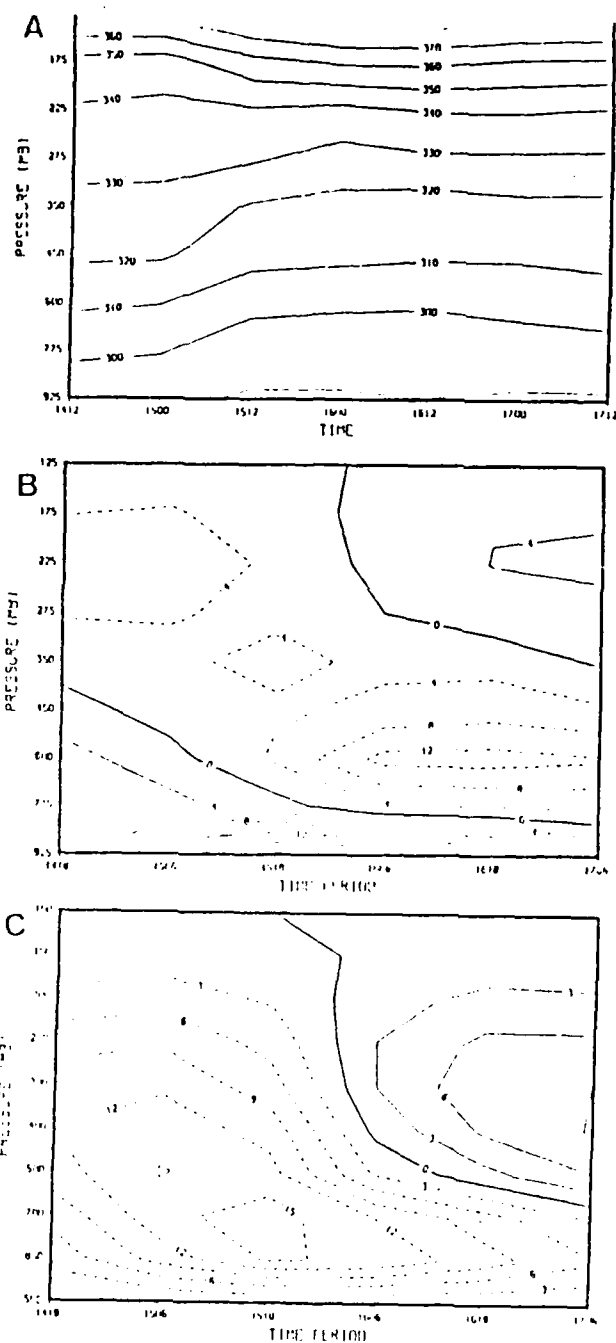
Fig. 28 Mass budget time sections (a) Area-average potential
temperature ($^{\circ}$K) for 6 deg radius budget volume, (b) lateral mass
transport (10^{12}gs^{-1} / 100 mb) and (c) kinematic vertical
velocities (10^{-7} mb s^{-1}). Dashed lines indicate divergence in
(b) and upward motion in (c). Time 1412 refers to 1200 UTC 14
December 1987.

44

atmosphere results in a net vertically integrated mass loss since the low-level convergence is concentrated only in the boundary layer. A vertically-integrated net mass gain occurs after 06 UTC 16 December (during the occlusion process) when upper level convergence is due to the merging of the two jet streaks, one over the eastern Pacific Ocean and the other over the southern Gulf of Alaska (Fig. 16).

The area-averaged kinematic vertical velocity (Fig. 28c) describes the vertical mass circulation. It shows initially strong upward motion in the mid-troposphere (300-500 mb) which further intensifies and lowers in height to 700 mb by 18 UTC 15 December. The maximum upward area average of omega 2 μb s^{-1} is found during the twelve hour period of maximum intensification. An upper tropospheric maximum of descent develops during the later stages of the cyclone. However, in the Calland and Cook studies, the maximum omega increased in height as the cyclone peaked in intensity. In this study, the upward vertical motions lowered as the cyclone peaked and then showed a significant decline in intensity by 06 UTC 16 December. This increased intensity in descending air in the middle and upper levels during the dissipation phase of the cyclone is attributable to the convergence in the jet streaks at 250 mb. The maximum upward velocities are comparable in magnitude to Cook and are about one half as intense as the values found by Calland.

C. Vorticity Budget Analysis

Fig. 29 presents six of the most important terms in the vorticity equation to illustrate the dynamics of the explosive cyclogenesis event of 14-17 December 1987. A time section of area-average vorticity ζ_a (Fig. 29a) describes the development
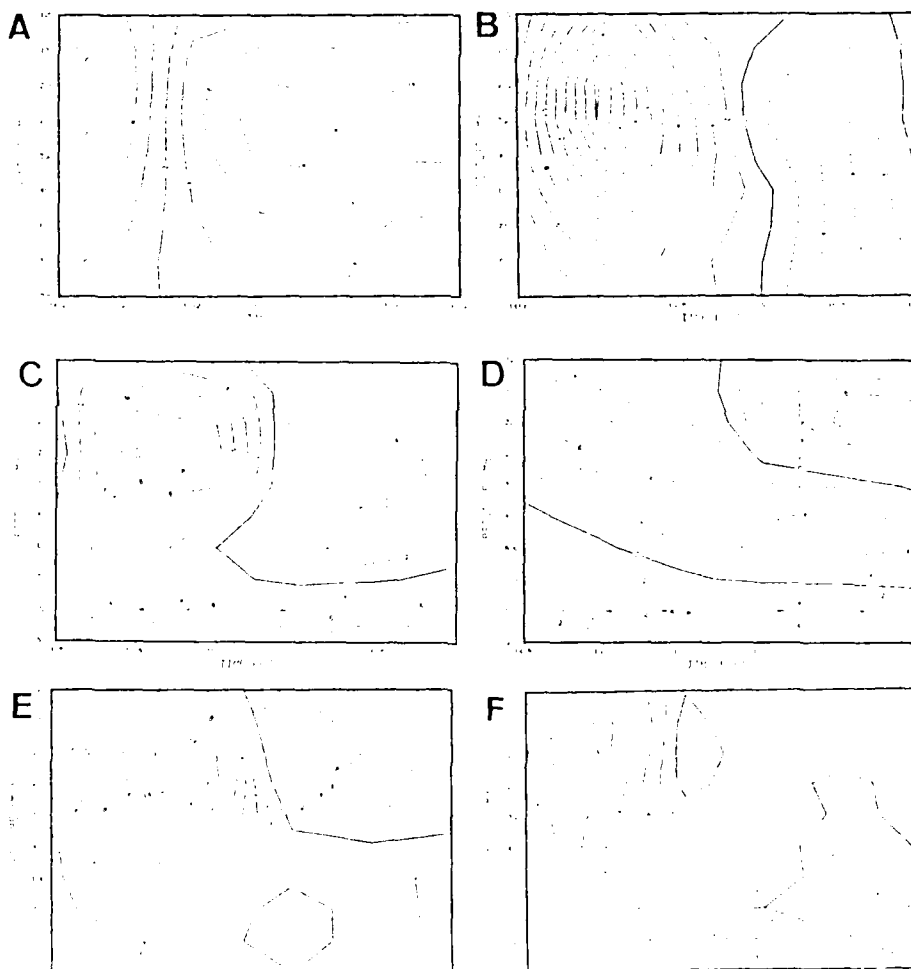
Fig. 29 Vorticity budget time sections (10^{-10} s^{-2}): (a) Area-average absolute vorticity time section; (b) time tendency; (c) lateral transport; (d) mean mode of lateral transport; (e) eddy mode of lateral transport; and (f) residual. Time 1418 refers to 1800 UTC 14 December 1987, the mid-point of the 12 h period 1200 to 0000 UTC.

sequence of this cyclone. As discussed in Fig. 2, four distinct evolutionary phases of the cyclone can be seen from the central pressure trace. Fig. 29a indicates these phases are present in the vorticity structure of the storm. Initially (open wave phase) weak cyclonic ζ_a (anticyclonic relative vorticity ζ) is present in upper (350-175 mb) and lower tropospheric (925-600 mb) layers. Then cyclonic ζ_a increases dramatically in all levels during the explosive cyclogenesis phase (30 h ending at 00 UTC 16 December) but is strongest at 500-250 mb. During the next 12 h, (mature phase) constant high values of ζ_a occurs at all levels with a maximum between 400-250 mb.

Finally, during the dissipation phase, ζ_a gradually decreases at all levels especially at the surface. The ζ_a time tendency (Fig. 29b) shows a time difference representation of Fig. 29a. Fig. 29b, presents an enormous increase in ζ_a (15 x $10^{-10}s^{-2}$) during the first 12 h of rapid cyclone development. The maximum increase is centered at 315 mb, slightly lower than in Calland's and Cook's studies. The increase in ζ_a is three times that of Calland and a third greater than Cook. During the dissipation phase, ζ_a became slightly negative throughout the entire atmosphere and resembles the pattern found by Calland and Cook.

The lateral vorticity transport in Fig. 29c is the summation of eddy mode and mean mode. Three distinct features dominate this time section. The first is the rapid increase in ζ_a at 275 mb during the first 12 h and reflects the influence that the

upper level short-wave trough has over the region. The second occurs at 925 mb during the period of most rapid intensification and coincides with the strongest mass inflow. The third feature is a weak negative ζ_a region above 775 mb and reflects the weakening of the surface cyclone and aloft as well.

The mean mode of lateral transport (Fig. 29d) reveals strong inward transport centered at 925 mb during the cyclone's most intense period and is consistent with the mass budget (Fig. 28b). Modest negative ζ_a above 400 mb descends in height to 600 mb as the system occludes. At the same time developing ζ_a centered near 275 mb reflects the interaction of the two jet streaks over the eastern Pacific Ocean.

The eddy mode of lateral transport (Fig. 29e) reveals large advection of ζ_a into the budget volume at 250 mb during 0000-1200 UTC 15 December when the surface low crosses north of the jet axis (cyclonic side) and entered into the divergent region of the jet (Fig. 10 and Fig. 16). When the jet streak from the Gulf of Alaska merges with the eastern Pacific Ocean jet streak, convergence aloft results (after 06 UTC 16 December). This feature was not observed in Calland and Cook. The near neutral advection in the lowest levels throughout the cyclone's life and maximum values of large cyclonic advection aloft were also observed in Calland and Cook.

The residual term (Fig. 29f) contains relatively weak sources of ζ_a throughout the time section. A modest $8 \times 10^{-10} s^{-2}$ value in the upper troposphere during the early time periods may

reflect inconsistencies in the placement and intensity of the CVA. During the later periods, a similar modest value exists and may be the result of the over intensification of the frictional dissipation near the surface.

The 6° budget volume generally represented the average between the 4° and 8° budget volumes which were +/- 50% of the 6° values, respectively. The budget residual time section (not shown) shows positive ς_a values under ($11 \times 10^{-10}s^{-2}$) in the upper and lower troposphere with a small area of negative ς_a values after 18 UTC 16 December, which are confined to 875-750 mb. The exact cause for these concentrated residuals are uncertain but may be linked to the course NMC grid point data fields. The 4° budget volume calculates residuals in excess of ($28 \times 10^{-10}s^{-2}$) while the 8° budget volume shows a similar structure as in Fig. 29b but with half the magnitude. However, the 6° budget volume's modest magnitudes are comparable to the results in Calland and Cook and provide confidence in the budget diagnostics.

D. Summary

The reliability of the budget analyses rest squarely on the accuracy of the grid point data fields. As was discussed in Section 2, the pre-explosive cyclogenesis phase of this storm was poorly analyzed. There were repeated inconsistencies in the position and intensity of the short wave trough and CVA region over the eastern Pacific Ocean as analyzed by NMC when compared

to satellite imagery. As a consequence, the budget results must be viewed with caution. It is interesting to note that the budget calculations still resulted in large ζ_a advection at upper levels despite the seemingly weak depiction of these features on the final analyses. It can only be concluded that if more detailed and accurate analyses were available for this study, the results would show an even stronger ζ_a advection pattern. Striking differences between this budget analysis and the studies by Calland and Cook can be explained by the vigorous upper level short-wave trough and jet streak dynamics absent in the other explosive events.

Statistics from the mass budget analysis show that the explosive cyclogenesis event is characterized by an initially well established mass circulation with low-level convergence and upper level divergence pattern. As the cyclone reaches maturity, the LND descends from 400 mb to 800 mb and the maximum divergence strengthens as it descends to 600 mb. During the period of rapid cyclogenesis, strong cooling below 275 mb occurs. This is consistent with the measured decrease in SI which approaches the moist adiabatic lapse rate. Rapid deepening of the surface low coincided with its entering the divergent front quadrant of the jet streak (Fig. 10 and Fig. 16) and the approach of the short-wave trough at 500 mb (Fig. 11 and Fig. 15). As the cyclone occludes, the maximum omega velocities rapidly decrease and the net vertically-integrated mass gain occurs.

The evaluation of the most important vorticity budget terms shows the increase of ζ_a tendency in the upper troposphere is caused by the advection of cyclonic vorticity. Total lateral transport shows maximum ζ_a rapidly increasing at 275 mb during the first 12 h of development then rapidly increasing at 925 mb during the next 12 h. Gradual decrease in ζ_a occurs after the cyclone occludes. Frictional dissipation helps deplete ζ_a in the lowest layer.

III. CONCLUSIONS

A. Summary

The synoptic discussion of the explosive cyclogenesis event that occurs over the eastern Pacific Ocean on 14-17 December 1987 is investigated using NMC objective analyses and digital satellite imagery.

As was shown in Section 1, a number of different physical processes determine to what extent an explosive event will occur. In most studies, three requisites for rapid cyclogenesis are suggested. They include: (1) an upper-level cyclonic vorticity center advecting towards; (2) a pre-existing low-level cyclone; and that (3) a favorable environment exists to couple (superposition) the low-level cyclone and the upper level jet streak or short-wave trough. This latter condition contains non-linear effects which are strongly determined by cyclogenesis regions (eastern verses western oceans).

In Section 2, it was shown that as an explosive low pressure center moves off the Asian continent, rapid intensification in meridional flow aloft occurs down stream across the entire Pacific Ocean. Building of the mid-Pacific Ocean 500 mb ridge allows Arctic air to advance to the mid-latitudes and assists in the formation of a jet streak over the southern Gulf of Alaska. Simultaneously, intensification of the 500 mb short-wave trough just upstream of the developing eastern Pacific Ocean cyclone occurs. As the surface low crosses to the cyclonic side of the jet streak, rapid cyclogenesis occurs. Rapid growth in the head

52

cloud northeast of the surface low during the explosive phase of development suggests an increase in convection is due to significant destabilization in the troposphere as a whole.

Despite relatively minor differences in the FNOC and NMC initial analyzed fields, the NOGAPS 3.0 and NGM models both failed to adequately capture the explosive event. Poor initialization over the data void mid-oceanic region is suggested as a plausible explanation for this failure.

The quasi-Lagrangian budget evaluation in Section 3 supports the synoptic observations in Section 2. The mass budget volume indicates that a strong low-level convergence (inflow) and upper level divergence (outflow) pattern is well established during the open wave phase of the surface cyclone and further intensifies until the occlusion process occurs. Rapid cooling in the mid troposphere during the explosive phase further destabilizes the atmosphere and is supported by the decrease in the 1000-500 mb area-average potential temperature lapse rates. The maximum upward vertical velocities reach their greatest magnitude at the time the cyclone attains minimum SLP and is consistent with the mass budget calculations. The continuous decrease in height of the LND appears to be unique to this explosive event but may be related to the merging of jet streaks over the cyclone during its dissipation phase. The vorticity statistics clearly show the importance of the upstream upper level short-wave which rapidly advects a huge quantity of cyclonic vorticity into the cyclone. The explosive event though not as intense as in the Reed and

Albright case still yielded similar characteristics. They

include:

1. Incipient cyclones were located within a strong and wide
   baroclinic zone;

2. The area average static stability levels decreased in
   vicinity of the storm approaching conditional instability.
   The explosive phase coincided with the surface low entering
   the divergent favored side of the jet streak;

3. Satellite imagery showed a rapid expansion of the cloud
   head and strong subsidence in the rear of the storm during
   the onset of the explosive phase;

4. The storm track nearly paralled the SST isotherms with only
   moderate temperature gradients existing along the path;

5. Maximum reported surface winds were $30ms^{-1}$;

6. Rapid cyclogenesis occurred in relatively infrequent
   regions for development;

7. The NWP models failed to forecast this event.

The differences found in this case as compared to Reed and
Albright include:

1. Cyclogenesis occurred under a strong upper level CVA
   region;

2. The jet streak in the vicinity of the surface low was 30
   ms^{-1} less intense;

3. Less low-level cold air advection was evident in the
   initial development of the low;

4. The Junker and Haller satellite classification was less
   useful with this storm.

B. **Recommendations**

A review of all operational data bogusing criteria is deemed

appropriate in view of the relative frequency and destructive

nature of explosive cyclogenesis. Careful screening of limited

oceanic synoptic data in regions conducive to superposition of

surface and upper level disturbances should be weighed on the

side of caution. Suggested signatures of an impending explosive event, such as reported 3-h pressure falls in excess of 6 mb which occur over a large region down stream of a surface low or rapid expansion of the cloud head in the vicinity of the surface low, could be used in the objective data assimilation decision process. Future research effects are required to develop a better relationship between budget results and central pressure changes that accompany explosive events.

LIST OF REFERENCES

Anthes, R.A., Y.-H. Kuo and J.R. Gyakum, 1983: Numerical simulations of a case of explosive marine cyclogenesis. Mon. Wea. Rev., 111, 1174-1188.

Bosart, L.F., 1981: The Presidents' Day snowstorm of 18-19 February 1979: A sybsynoptic-scale event. Mon. Wea. Rev., 109, 1542-1566.

Bosart, L.F. and S.C. Lin, 1984: A diagnostic analysis of the Presidents' Day storm of February 1979. Mon. Wea. Rev., 112, 2148-2177.

Bottger, H., M. Eckardt and U. Katergiannakis, 1975: Forecasting extratropical storms with hurricane intensity using satellite informaiton. J. Appl. Meteor., 14, 1259-1265.

Calland, W.E., 1983: Quasi-Langrangian diagnostics applied to an extratropical explosive cyclogenesis in the North Pacific. Master's Thesis, Department of Meteorology, Naval Postgraduate Schoo, Monterey, Ca 93943, 154 pp.

Carlson, T.N., 1980: Airflwo through midlatitude cyclones and the ocmma cloud pattern. Mon. Wea. Rev, 108, 1498-1509.

Cook, W.A., 1983: A quasi-Langrangian diagnostics investigation of rapid cyclones in a polar air stream. Master's Thesis, Department of Meteorology, Naval Postgraduate School, Monterey, CA 93943, 144 pp.

Gyakum, J.R., 1983a: On the evolution of the QE II storm. I: Synoptic aspects. Mon. Wea. Rev, 111, 1137-1155.

Gyakum, J.R., 1983b: On the evolution of the QE II storm. II: Dynamics and thermo-dynamic structure. Mon. Wea. Rev, 111, 1156-1173.

Hales, J.E., 1979: A subjective assessment of model initial conditions using satellite imagery. Bull. Am. Meteor. 60, 206-211.

Holland, G.J., A.H. Lynch and L.M. Leslie, 1987: Australian East-Coast cyclones. Part I:Synoptic overview and case study. Mon. Wea. Rev, 115, 3024-3036.

Johnson, D.R., and W.K. Downey, 1975: Azimuthally averaged transport and budget equations for storms: Quasi-Langrangian diagnostics 1. Mon. Wea. Rev, 103, 967-979.

Johnson, D.R. and C.H. Wash, 1979: Dynamical verification of numerically simulated extratropical cyclogenesis using quasi-Langrangian diagnostics. Reprints Fourth Conf. on Numerical Weather Prediction, Amer. Meteor. Soc., 144-150.

Junker, N.W., and D.J. Haller, 1980: Estimation of surface pressures form satellite cloud patterns. Mar. Wea. Log, 24, 83-87.

Kuo, Y.H. and R.J. Reed, 1988: Numerical simulation of an explosively deepening cyclone in the eastern Pacific. Mon. Wea. Rev, 116, in press.

Leslie, L.M., G.J. Holland and A.H. Lynch, 1987: Australian East-Coast cyclones. Part II: Numerical modeling study. Mon. Wea. Rev, 115, 3037-3054.

Liou, C.-S. and R.L. Elsberry, 1987: Heat budgets of anlayses and forecasts of an explosively deepening maritime cyclone. Mon. Wea. Rev, 115, 1809-1824.

Ludlum, D.M., 1988: Weatherwatch. Weatherwise, 41, 119-120.

Mullen, S.L., 1983: Explosive cyclogenesis associated with cyclones in polar air streams. Mon. Wea. Rev, 111, 1537-1553.

Murty, T.S., G.A. McBean and B. McKee, 1983: Explosive cyclogenesis over the northeast Pacific Ocean. Mon. Wea. Rev, 111, 1131-1135.

Namias, J., 1987: Factors relating to the explosive North Atlantic cyclone of December 1986. Wea. 42, 322-325.

National Oceanic Atmospheric Administration, 1987: Storm Data, 29, Number 4, National Climatic Data Center, Federal Building, Asheville, NC 28801.

National Oceanic Atmospheric Administration, 1987: Storm Data, 30, Number 1, National Climatic Data Center, Federal Building, Asheville, NC 28801.

Pettersen, S. and S.J. Smebye, 1971: On the development of extratropical cyclones. Quart. J. Roy. Meteor. Soc., 97, 457-482.

Reed, R.J., and M.D. Albright, 1986: A case study of explosive cyclogenesis in the eastern Pacific. Mon. Wea. Rev, 114, 2297-2319.

Roebber, P.J., 1984: Statistical analysis and updated climatology of explosive cyclones. <u>Mon. Wea. Rev</u>, <u>112</u>, 1577-1589.

Rogers, E., and L.F. Bosart, 1986: An investigation of explosively deepening oceanic cyclones. <u>Mon. Wea. Rev</u>, <u>114</u>, 702-718.

Sanders, F., 1986a: Explosive cyclogenesis over the west-central North Atlantic Ocean. 1981-1984. Part I: Composite structure and mean behavior. <u>Mon. Wea. Rev</u>, <u>114</u>, 1781-1794.

Sanders, F., 1986b: Explosive cyclogenesis over the west-central North Atlantic Ocean. 1981-1984. Part II: Evaluation of LFM model performance. <u>Mon. Wea. Rev</u>, <u>114</u>, 2207-2218.

Sanders, F., 1987a: A study of 500 mb vorticity maxima crossing the east coast of North America and associated surface cyclogenesis. <u>Wea. Forecasting</u>, <u>2</u>, 70-83.

Sanders, F., 1987b: Skill of NMC operational dynamical models in prediction of explosive cyclogenesis. <u>Wea. Forecasting</u>, <u>2</u>, 322-336.

Sanders, F., and J.R. Gyakum, 1980: Synoptic-dynamic climatology of the "bomb". <u>Mon. Wea. Rev</u>, <u>108</u>, 1589-1606.

Soper, D.J., 1987: Diagnostic study of a genesis of Atlantic lows experiment (GALE) cyclogenesis event. Masters's Thesis, Department of Meteorology, Naval Postgraduate School, Monterey, CA 93943, 138 pp.

Uccellini, L.W., 1986: The possible influence of upstream upper-level baroclinic processes on the development of the QE II storm. <u>Mon. Wea. Rev.</u>, <u>114</u>, 1019-1027.

Uccellini, L.W., D. Keyser, K.F. Brill and C.H. Wash, 1985: The Pesidents' Day cyclone of 18-19 February 1979: Influence of upstream trough amplification and associated tropopause folding on rapid cyclogenesis. <u>Mon. Wea. Rev.</u>, <u>113</u>, 962-988.

Uccellini, L.W., P.J. Kocin, R.A. Petersen, C.H. Wash and K.F. Brill, 1984: The Presidents' Day cyclone of 18-19 February 1979: Synoptic overview and analysis of the subtropical jet streak influencing the pre-cyclogenetic period. <u>Mon. Wea. Rev.</u>, <u>112</u>, 31-55.

Uccellini, L.W., R.A. Petersen, K.F. Brill, P.J. Kocin and J.J. Tuccillo, 1987: Synergistic interactions between and upper-level jet streak and diabatic processes that influence the development of a low-level jet and a secondary coastal cyclone. <u>Mon. Wea. Rev</u>., <u>115</u>, 2227-2261.

Wash, C.H., J.E. Peak, W.E. Calland and W.A. Cook, 1988: Diagnostic study of explosive cyclognesis during FGGE. <u>Mon. Wea. Rev</u>., <u>116</u>, 431-451.

INITIAL DISTRIBUTION LIST

No. Copies

1. Defense Technical Information Center 2
   Cameron Station
   Alexandria, VA 22304-6145

2. Library, Code 0142 2
   Naval Postgraduate School
   Monterey, CA 93943-5002

3. Chairman (Code 63Rd) 1
   Department of Meteorology
   Naval Postgraduate School
   Monterey, CA 93943-5000

4. Chairman (Code 68Co) 1
   Department of Oceanography
   Naval Postgraduate School
   Monterey, CA 93943-5000

5. Professor Carlyle H. Wash (Code 63Wx) 5
   Department of Meteorology
   Naval Postgraduate School
   Monterey, CA 93943-5000

6. Professor R.L. Elsberry (Code 63Es) 1
   Department of Meteorology
   Naval Postgraduate School
   Monterey, CA 93943-5000

7. Professor Wendell A. Nuss (Code 63Nu) 1
   Department of Meteorology
   Naval Postgraduate School
   Monterey, CA 93943-5000

8. LCDR J. Curtis, USN 1
   19325 Robin Hood Way
   Monument, CO 80132-8754

9. Director Naval Oceanography Division 1
   Naval Observatory
   34th and Massachusetts Ave., NW
   Washington, DC 20390

10. Commander 1
    Naval Oceanography Command
    NSTL Station
    Bay St. Louis, MS 39522

11. Commanding Officer   1
    Naval Oceanographic Office
    NSTL Station
    Bay St. Louis, MS 39522

12. Commanding Officer   1
    Fleet Numerical Oceanography Center
    Monterey, CA 93943

13. Commanding Officer   1
    Naval Environmental Prediction Research Facility
    Monterey, CA 93943

14. Chairman, Oceanography Department   1
    U.S. Naval Academy
    Annapolis, MD 21402

15. Chief of Naval Research   1
    800 North Quincy Street
    Arlington, VA 22217

16. Office of Naval Research (Code 420)   1
    Naval Ocean Research and Development Activity
    800 North Quincy Street
    Arlington, VA 22217